COMBINED MICRO AND NANOPATTERNING FOR CELL SUBSTRATES

A Thesis
Presented to
The Academic Faculty

by

Marcus T. Eliason

In Partial Fulfillment
of the Requirements for the Degree
Master of Science in the
Woodruff School of Mechanical Engineering

Georgia Institute of Technology
May 2007

COMBINED MICRO AND NANOPATTERNING FOR CELL SUBSTRATES

Approved by:

Dr. William P. King, Advisor
School of Mechanical Engineering
Georgia Institute of Technology

Dr. Andrés J. García
School of Mechanical Engineering
Georgia Institute of Technology

Dr. Samuel Graham
School of Mechanical Engineering
Georgia Institute of Technology

Date Approved: April 2007

ACKNOWLEDGEMENTS

"The science you don't know looks like magic." This is a quote by one of my favorite authors, Christopher Moore, in his book Fluke. It is something that I scribbled in my first lab notebook to use as inspiration. Although the science part has frustrated me many times during graduate school and magic has seemed like a much better explanation for my experiments, I do consider the understanding of the science a much more worthy pursuit. But as the author of that quote later said, he preferred the magic explanation because it generally involves less math. Anyone who has seen my math grades over the years can understand why this statement is something I can completely agree with.

I would like to start off by thanking the members of my committee. Your help and guidance throughout this process have been invaluable in shaping my research. I thank Dr. Garcia and his lab, especially Kristin Michael, Lindsay Bryant, Kellie Burns, Sean Coyer and Tim Petrie for helping a lowly mechanical engineer 8 years removed from a biology class understand what was actually going on in my experiments as well as technical support. I thank Dr. Graham for his assistance with carbon nanotubes as well as his student Erik Sunden who grew the carbon nanotubes used in part of this work. A special thank you goes out to the rest of Dr. Graham's group for many laughs from the office across the hall.

I owe the biggest thank you to my advisor, Dr. Bill King, for his guidance and support during my time in graduate school. Without these I feel I would have missed out on a great opportunity. I would like to thank my fellow members of the NTPL, including Brent, Harry, Fabian, Andrew, Jay, Shubham, Keunhan, and Tänya. A special thank you

goes to Joe Charest for his help in shaping my research from the beginning when I started as an undergraduate. I thank you all for laughs, rants, scowls, and couches to sleep on. I realize I might not have always been one of the best graduate students, but hopefully I wasn't one of the worst.

Finally, I would like to thank my family for their support during this time and always providing me with a comfy bed to come home to when school became too frustrating. I always remember your advice of "take it easy, but study hard," and hopefully I have found the happy medium between the two.

TABLE OF CONTENTS

LIST OF FIGURES

SUMMARY

The success of many emerging biotechnologies depends upon the ability to tune cell function to mimic conditions found *in vivo*. Cells exhibit complex interactions with their surrounding environment known and the extracellular matrix (ECM). These interactions control many cell functions such as proliferation, differentiation and cell death. ECM components span the meso-, micro- and nano-length scales. Successful biotechnologies therefore must also exhibit patterning over these length scales.

The objective of this study is to fabricate and analyze cell response to micro and nanopatterned polymer substrates. Experiments examined cell alignment and proliferation to various substrates. The substrates used featured micropatterned grooves and holes, micropatterned carbon nanotubes, and combinations of microgrooves and nanogrooves. Results showed significant interactions between cell alignment and the patterned topography for all substrate types, while cell proliferation showed no significant dependence on these topographic parameters.

CHAPTER 1

INTRODUCTION

1.1 Introduction

Emerging biotechnologies, biomaterials, and tissue engineering constructs face many obstacles before successful implementation. One such challenge is how to fabricate an *ex vivo* construct to ellicit a specific cell response *in vivo*. Cell responses are highly environment dependent so an accurate model of *in vivo* conditions is necessary for success. This thesis presents methods for fabricating polymer cell substrates with complex patterns spanning multiple length scales to better understand cell response to environmental cues.

Cells exhibit highly sensitive interactions with the surrounding environment of topography and chemistry. Many cell functions such as proliferation, differention and apoptosis are influenced from cues found in the extracellular matrix (ECM). Understanding these cues is necessary to direct a desired cell response. Achieving a desired response will enhance the likelihood of successful biotechnologies. Early work into cell response to patterned substrates showed that topography can influence cell orientation and growth[1,2]. These studies however focused solely on micropatterned substrates. More recent work has been done to look at the effects of nanopatterned[3] and chemically patterned substrates[4,5]. Reviews of cell and surface topographic interactions are available which discuss the key aspects of the cellular responses[6,7].

Investigations into cell responses to patterned substrates have been performed on a variety of materials[6]. The majority however utilize silicon, glass, or polymers. Of these materials, polymers offer an easier and cheaper route to micro and nanopatterning. Silicon substrates can easily be manufactured using standard photolithography techniques. These processes, however, require expensive equipment and rigorous protocols to achieve uniform patterns over many samples. Substrates made of glass face similar processing issues. Polymers however do not suffer from the same processing disadvantages. Material properties of polymers can easily be tuned to a desired design. Polymers also have better biocompatibility with some already FDA approved for *in vivo* use making them attractive to future biotechnologies. Most polymer substrates are fabricated using casting[8] or embossing processes[9]. Casting processes involve a liquid polymer poured onto a master, cured, and removed from the master. Casting processes are limited to polymers that can be cured and released from a master. Embossing or imprint lithography can be used with a wider range of polymers. In this process a patterned master is brought into contact with a polymer substrate under heat and force. After cooling and removal of load, the master is removed leaving replicate features in the polymer. Figure 1.1 shows a schematic of the hot embossing process, and Figure 1.2 shows a typical silicon master and embossed feature replicate. Many embossed replicates can be fabricated form a single patterned master, lowering the cost and processing time for many replicates. Imprint lithography also has already shown the ability to fabricate features with millimeter scale down to 10 nm[10]. Many studies have successfully utilized embossed substrates for studies of cell response analysis.

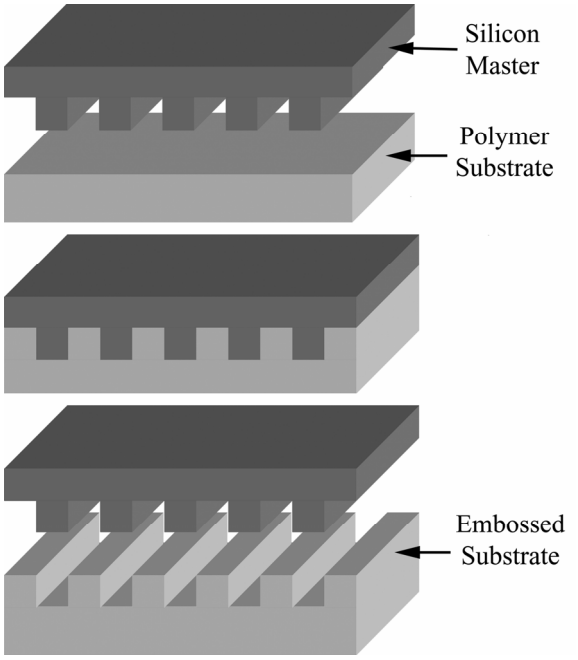

Figure 1.1. Schematic of the hot embossing lithography process.

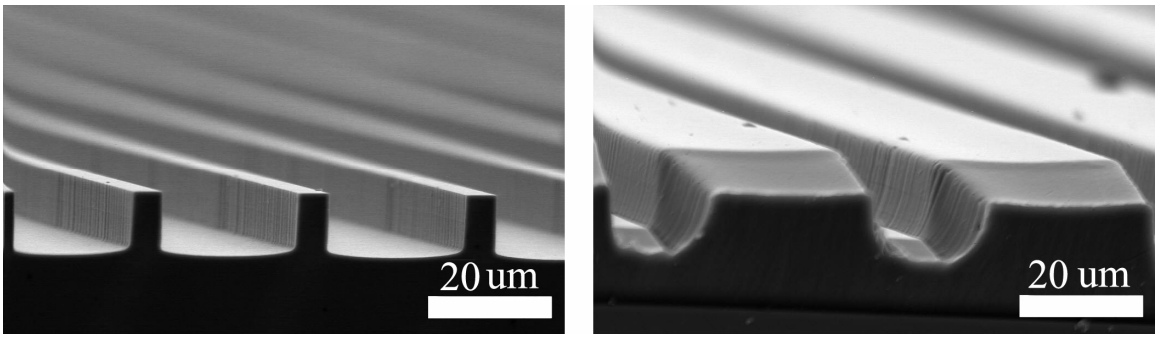

Figure 1.2. Scanning electron micrographs of (left) silicon micromachined master and (right) embossed polymer replicate.

This thesis describes the fabrication of polymer cell substrates and the analysis of cell response to these substrates. The work centers on three types of substrates spanning the micro- and nano-length scales. The first type of substrate consisted of micropatterned grooves and holes with spacings of 1 to 75 μm and depths of 1 and 5 μm. All of the patterns were on a single substrate to limit sample variability and to conduct experiments

in a high-throughput fashion. Alignment and proliferation were analyzed on cells cultured on these substrates. The second type of substrate featured micrpatterns of carbon nanotubes. The nanotube features of lines and circles had spacings from 9 to 76 μm on a single substrate to analyze cell alignment to many different pattern types at once. The final type of substrate used in this work had combinations of micropatterns and nanopatterns. Microgrooves were first formed into polymer substrates followed by the fabrication of nanogrooves on top of the micomesas. Samples were fabricated with nanogrooves in parallel and perpendicular to the microgrooves. Cell alignment was tested to these substrates. Results showed significant interactions between cell alignment and the patterned topography for all substrate types, while cell proliferation showed no significant interactions.

1.2 References

1. Rovensky YA, Slavnaja IL, Vasiliev JM. Behaviour of Fibroblast-Like Cells on Grooved Surfaces. Experimental Cell Research 1971;65(1):193-&.

2. Weiss P. Experiments on Cell and Axon Orientation In Vitro: The Role of Colloidal Exudates in Tissure Organization. Journal of Experimental Zoology 1945(100):353-386.

3. Yim EKF, Reano RM, Pang SW, Yee AF, Chen CS, Leong KW. Nanopattern-induced changes in morphology and motility of smooth muscle cells. Biomaterials 2005;26(26):5405-5413.

4. Charest JL, Eliason MT, Garcia AJ, King WP. Combined microscale mechanical topography and chemical patterns on polymer cell culture substrates. Biomaterials 2006;27(11):2487-2494.

5. Charest JL, Eliason MT, Garcia AJ, King WP, Talin AA, Simmons BA. Polymer cell culture substrates with combined nanotopographical patterns and micropatterned chemical domains. Journal of Vacuum Science & Technology B 2005;23(6):3011-3014.

6. Flemming RG, Murphy CJ, Abrams GA, Goodman SL, Nealey PF. Effects of synthetic micro- and nano-structured surfaces on cell behavior. Biomaterials 1999;20:573–588.

7. Stevens MM, George JH. Exploring and engineering the cell surface interface. Science 2005;310(5751):1135-1138.

8. Clark P, Connolly P, Curtis ASG, Dow JAT, Wilkinson CDW. Topographical Control of Cell Behavior .1. Simple Step Cues. Development 1987;99(3):439-448.

9. Charest JL, Bryant LE, Garcia AJ, King WP. Hot embossing for micropatterned cell substrates. Biomaterials 2004;25(19):4767-4775.

10. Chou SY, Krauss PR. Imprint lithography with sub-10 nm feature size and high throughput. Microelectronic Engineering 1997;35(1-4):237-240.

CHAPTER 2

THE IMPACT OF CELL SUBSTRATE MICROTOPOGRAPHY ON CELL ALIGNMENT AND PROLIFERATION INVESTIGATED USING A HIGH THROUGHPUT CHIP

This chapter reports the use of a high-throughput chip to study the impact of microtopography on osteoblast-like cell alignment and proliferation. Topographic patterns on polymer substrates were fabricated using hot embossing to press the micropatterned features of a Ni master onto a polymer substrate at elevated temperature. The resulting 1x1 cm cell culture substrates contained 35 distinct micropatterns of grooves and holes, with characteristic feature sizes ranging from 1 to 75 μm. The feature depths were either 1 or 5 μm. Osteoblast-like cells were cultured on the chips and cell response was examined using fluorescence and electron microscopy. The influence of the micropatterns on cell alignment and proliferation was quantified. Cell alignment showed very strong responses to micropatterns with a maximum alignment to microgrooves of 94 ± 1.6%. Cell proliferation, however, did not exhibit any significant dependence to the varying micropatterns. The high-throughput technique developed here allows for cell response to be examined over many different patterns. Overall, 64 separate experiments were run on more than 12,000 cells on a single chip, indicating the usefulness of this high-throughput technique.

2.1 Introduction

An understanding of cell-surface interactions is crucial for the advancement of biomaterials and biomedical devices, biotechnological platforms, and tissue engineered constructs. Surfaces with microtopographies can have a large impact upon a number of cell functions. This chapter presents a method to analyze cellular responses to microtopographies using a single chip that has 35 separate microtopographical regions. The alignment and proliferation of osteoblast-like cells are examined on the high-throughput chip.

Cell function, including morphology and orientation of adherent cells, is influenced by the substrate upon which the cells are attached. The size and shape of features present on the substrate can have a large impact on cells[1-4]. Many studies have shown cellular responses to microtopographies utilizing various materials such as silicon, glass, and polymers. A review of cell and surface topographic interactions is available which discusses the key aspects of the cellular responses[3]. Of the substrate materials typically used, polymers are often desirable due to their lower cost, ease of processing, and tunable material properties. Microtopographical cell substrates fabricated from silicon require a significant investment in time and machinery to fabricate a large number of substrates. Microtopographical polymer substrates offer an easier and less expensive path to fabrication, since costly, complex machinery is not needed.

Microtopography can be produced in a polymer cell substrate using either casting[5] or embossing[6]. Casting processes involve a liquid polymer poured onto a master, cured, and removed from the master. This approach has been widely used to fabricate microtopographical cell substrates to study interactions between cells and the

patterned polymers[5,7-17]. By nature of the casting process, polymer choice is limited to polymers that once cured can be released from the master. Embossing or imprint lithography, however, offers a wider range of materials as microtopographical features can be formed in nearly any thermoplastic polymer. In embossing-based fabrication, a master template is brought into contact with a polymer layer under heat and force to create a negative of the master features. This process can form features of sizes from less than 10 nm up to millimeter scale[18]. Imprint lithography has been used to fabricate cell culture substrates with low cost, high speed, and good repeatability[1,19,20].

While previous studies have examined the impact of microtopography on cell functions, most are limited to a small number of patterns and sizes[2,5,7-17,21,22]. Typically, between 1 and 6 patterns are tested in any one experiment. Because the sample fabrication and analysis are serial in nature, usually 100-500 cells are tested in any one set of experiments, and rarely more than 1,000 cells are tested. Furthermore, when single pattern substrates are used, there can be variability in the experiments from small changes in processing parameters during fabrication and differences in cell culture conditions. A comprehensive analysis of cell response to topography requires a large range of pattern types and sizes, a large number of cells per pattern, and strict controls on substrate fabrication that limit variability. The present chapter uses a single chip with many different patterns fabricated in parallel to minimize sample variability and comprehensively analyze a wide spectrum of patterns for cell alignment and proliferation.

This chapter describes a method for creating micropatterns using imprint lithography[1,6] for high throughput cell analysis. Polycarbonate (PC) substrate chips were fabricated with 35 distinct micropatterns with feature sizes ranging from 1 to 75 μm

and depths of 1 and 5 μm. Of the 35 patterns present on the chip, 16 were utilized during this experiment. Substrates were treated to create a uniform surface chemistry[23,24] and MC3T3-E1 osteoblast-like cells incubated for 20 hours. Cells were examined with fluorescence and scanning electron microscopy for alignment and proliferation. Results showed strong interactions between cellular alignment and topography but no significant interactions between proliferation and topography.

2.2 Materials and Methods

Hot embossing was used to fabricate substrates for cellular analysis. The alignment and proliferation were analyzed on greater than 40 cells per field grown on microtopographies having holes and grooves, with feature sizes in the range of 5 to 75 μm. Fluorescence and scanning electron microscopy was used to analyze cell alignment, and BrdU incorporation was used as a measure of proliferation.

2.2.1 Substrate Fabrication

Polymer cell substrate microtopographies were formed using a hot embossing process as demonstrated by our group previously[1]. Figure 2.1 shows a schematic of this process in which a micropatterned master is brought into contact with a polymer layer with heat and force to produce relief microstructures.

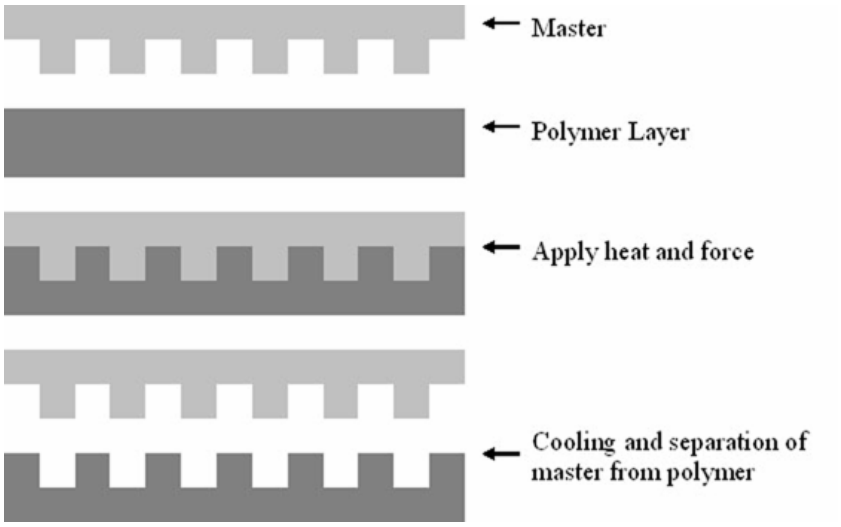

Figure 2.1. Schematic of the hot embossing process. A micromachined master is brought into contact with a polymer layer under heat and force. The system is then cooled and the replicate removed from the master.

Hot embossing was used because it can produce many polymer cell substrate replicates from one master. Hot embossing replication is easier and costs less than traditional silicon micromachining processes alone. The embossing masters were made of nickel and had micropatterns of lines and pillars with sizes ranging from 1 to 75 μm. Micropatterned features were formed in silicon using standard photolithography techniques and electroplated with nickel to create metal masters. Figure 2.2 provides an overview of pattern types and sizes present on the high-throughput chip as well as the patterns used in this work. The smallest pattern used was 5 μm followed by 7, 10, 15, 20, 30, 40, 50 and 75 μm. For microgroove patterns, the pattern number is the groove and mesa width, while for hole features the pattern number is the diameter of the hole with a one-half the center-to-center distance.

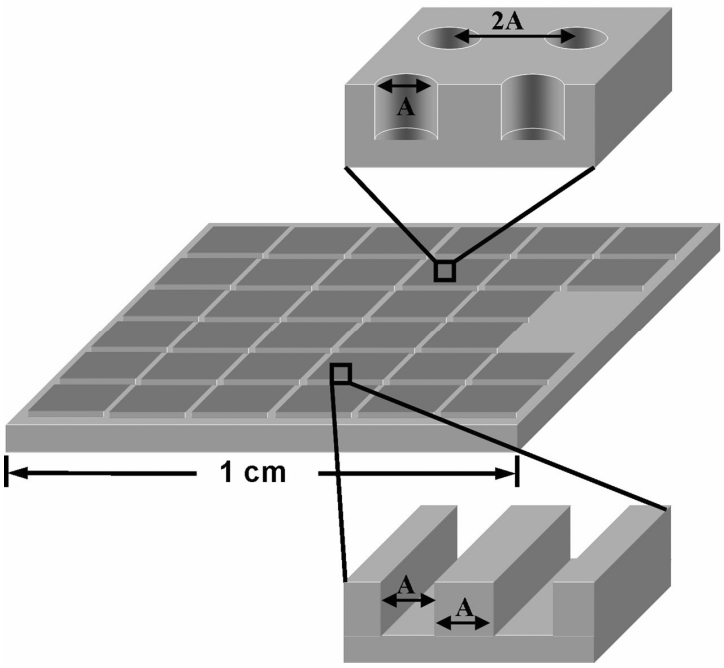

A (um)	Feature Type
Smooth	Line/Hole
1	
2	
3	
4	
5	Line/Hole
7	Line
10	Line/Hole
15	Line
20	Line/Hole
25	
30	Line/Hole
35	
40	Line/Hole
45	
50	Line/Hole
60	
75	Line/Hole

Figure 2.2. Overview of patterns present on the high-throughput chip. Chip includes 35 different patterns including a smooth surface for control measurements. Of the 35 patterns present, the 16 used are listed. Patterns referenced to as "Lines" are used for microgroove analysis and those with "Holes" for microhole analysis.

The polymer substrates were 0.5 mm thick polycarbonate (PC). The embossing was performed in a pressure and temperature controlled press. The press was heated to 166°C and the embossing stack inserted between the platens. The stack consisted of the PC sheet and Ni master sandwiched between 2 metal plates resting on a sheet of rubber to provide compliance. This stack arrangement was used to evenly distribute the load during the embossing step. The stack was heated to temperature and pressed with loads of up to 19 MPa. Samples were held at this temperature and pressure for one hour and then cooled to 37°C over ten minutes while under load. Once cooled to room temperature, the load was released and the stack removed from the press. The Ni master was removed leaving the micropatterned polymer replicate.

Substrate characterization was performed via optical and electron microscopy. Figure 2.3 shows an overview of the embossed chip as well as optical micrographs showing regions where multiple patterns of different sizes meet.

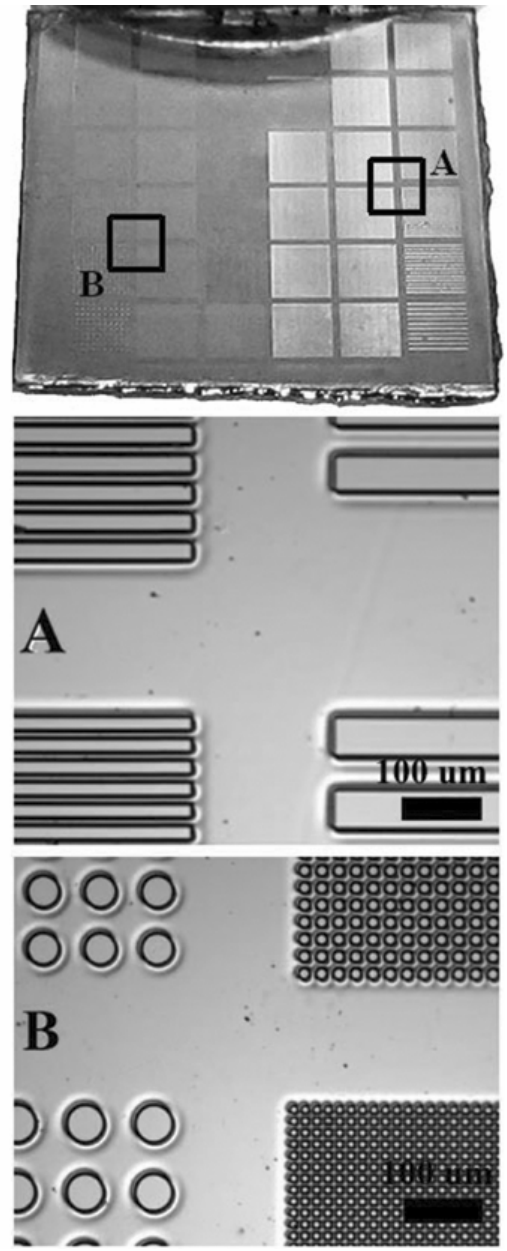

Figure 2.3. Image of embossed high-throughput sample. (**A**) and (**B**) images are optical micrographs showing embossed patterns in close proximity to each other (scale bars equal to 100 μm).

SEM analysis was also performed to verify feature spacing as well as depth. Figure 2.4 shows SEMs of 1 and 5 μm deep features. Pattern spacing was verified using measurement tools within the SEM. Feature depth had been previously tested by using profilometry and interferometry on the embossing masters and was consistent with depths seen in embossed replicates tested with AFM.

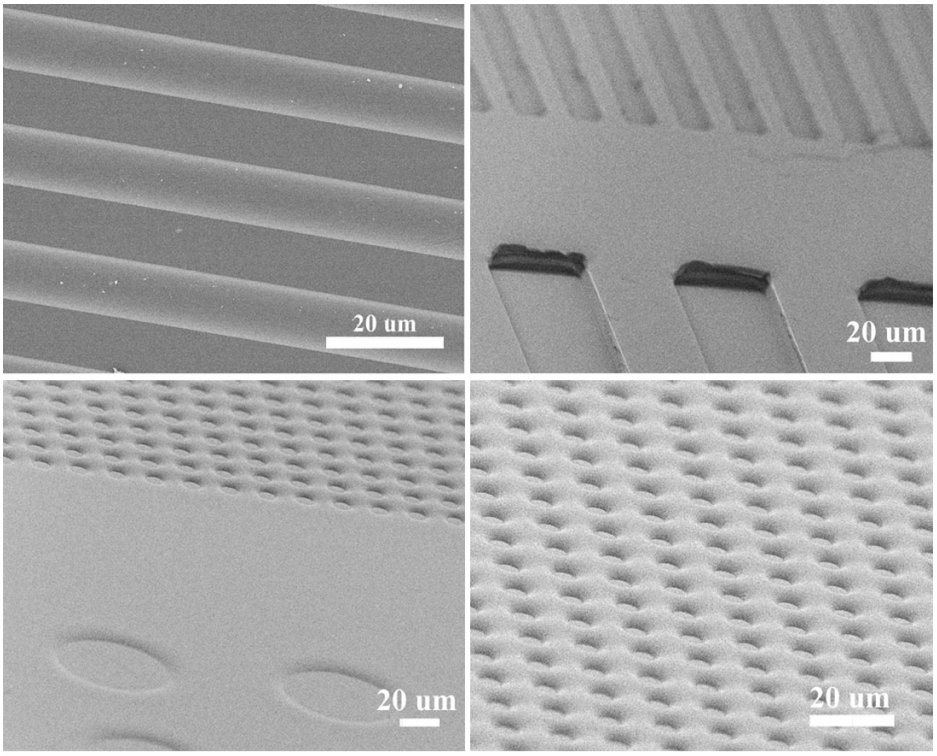

Figure 2.4. *Top Left*: SEM of 10x10 μm pattern. *Top Right*: SEM showing proximity of patterns on High-Throughput chip. Microfeatures are 5 μm deep. *Bottom Left*: SEM of embossed 1um deep holes in close proximity. *Bottom Right*: SEM of 7x7 μm embossed hole pattern. Scale bars for all micrographs equal to 20 μm.

2.2.2 Cell Culture

Embossed samples were cut into square chips 1 cm on a side and coated with 100Å thick Ti and 200Å thick Au using an electron-beam evaporator. Samples were immersed in hexadecanethiol (HDT) and dried under a nitrogen stream for 15 seconds to

create uniform surface chemistry. Next, samples were sterilized with three rinses in 95% ethanol and rinsed three times in PBS. Samples were then incubated in fibronectin (20 μg/mL in PBS) for 30 minutes as characterized previously[23,24]. After a 1 hour incubation in 1% heat denatured bovine serum albumin (BSA) at 37°C and 5% CO_2, MC3T3-E1 osteoblast-like cells were seeded at a density of 50 cells/mm^2. Cells were cultured in α-minimal essential medium with 10% fetal bovine serum and 1% penicillin-streptomycin and incubated at 37°C and 5% CO_2 [1]. Once cells were seeded, the samples were either used for alignment, proliferation, or SEM analysis.

2.2.3 Analysis

For alignment analysis, after 20 hours in culture, cells were permeabilized in 0.5% Triton X-100 cytoskeleton buffer (50 mM NaCl, 150 nM sucrose, 3mM $MgCl_2$, 50 mM tris(hydroxymethyl), 20 mg/mL aprotinin, and 1 mg/mL leupeptin , and 1 mM phenylmethylsulfonyl fluoride with pH of 6.8) for 5 minutes and fixed with 3.7% formaldehyde in PBS for 2 min. Samples were then blocked for 1-hour in 1% BSA. Next, samples were incubated in a primary antibody against fibronectin for 1 hour, rinsed twice in PBS, blocked in BSA for 10 minutes and followed with two more PBS rinses. Samples were incubated in secondary fluorochrome-labeled anti-IgG, rhodamine-phalloidin and Hoechst DNA stain for 1 hour, rinsed as before and mounted on glass slides. Samples were examined using a fluorescence microscope and processed using image analysis software. Alignment was determined using alignment of the cell nucleus. Each nucleus was fitted with an ellipse and the angle of the major axis of the ellipse recorded. Previous work has shown that the nuclear alignment angle is a good measure for overall cellular alignment[1]. After normalization to the micropattern angle, an

alignment angle ranging from 0-90° was obtained. Aligned cells are those considered to be within 10° of the micropatterns present on the substrate.

A proliferation assay was performed using BrdU. This thymidine analogue is incorporated into DNA during the synthesis phase of the cell cycle and is commonly used to determine cell proliferation. After 18 hours in culture, the normal culture media solution was replaced with a 3.1 μg/mL BrdU (Sigma) solution in culture media and incubated for an additional 4 hours. After rinsing in PBS, the cultures were fixed in 70% ethanol at 4°C for 10 minutes and denatured in 4M HCl for 20 minutes. The samples were then neutralized in 50 mM NaCl in 100 mM Tris-HCl (pH 7.4) for 15 minutes. Following rinsing in PBS, samples were incubated in 1% BSA for 30 minutes. The primary antibody against BrdU was then applied and allowed to incubate for 1 hour followed by rinsing in PBS and incubation in BSA for ten minutes. Samples were rinsed again with PBS and incubated in the secondary antibody of Alexa Fluor488-conjugated anti-mouse IgG and Hoechst DNA stain for 1 hour. Samples were then rinsed and mounted to glass slides. Analysis was performed using microscope equipped with fluorescence optics by scoring the number of BrdU positive cells over the total number of cell nuclei on a given sample. This protocol was a modification from the procedure previously developed by our group[25].

For SEM preparation, samples were rinsed twice in PBS and then fixed in 2.5% glutaraldehyde in PBS for 30 minutes at 4°C, then dried using graded ethanol series (70%, 90% and 100% ethanol) for 30 minutes each. Samples were then soaked twice in hexamethyldisilazane (HMDS) for 30 minutes each. Samples were then left to dry

overnight in a dessicator before sputter coating in gold and examination in a LEO 1530 SEM with an accelerating voltage of 3 kV.

2.2.4 Statistics

Experiments for cell alignment on 1 and 5 μm deep features were conducted independently with n = 5. Cell proliferation experiments were done independently as well with n = 3. Results are reported as mean ± standard error of the mean. Interactions were tested using a two-way ANOVA with depth and pattern as fixed variables using SYSTAT 8.0. *P*-values less than 0.05 were considered significant.

2.3 Results

A number of papers have analyzed the effects of microtopographies on cell function[2,3]. These studies mainly look at a small number of surface patterns and depths. The present work analyzes a large range of patterns and sizes on a single chip. The single chip approach enables identical culture conditions for the range of topographies examined, ensuring precise comparisons between fields resulting in a reduction in error.

Cellular alignment was determined by comparing the alignment of the cell nucleus with respect to the substrate topographic patterns. Figure 2.5 shows representative images of cell nuclei on a flat control surface and a microgroove patterned surface.

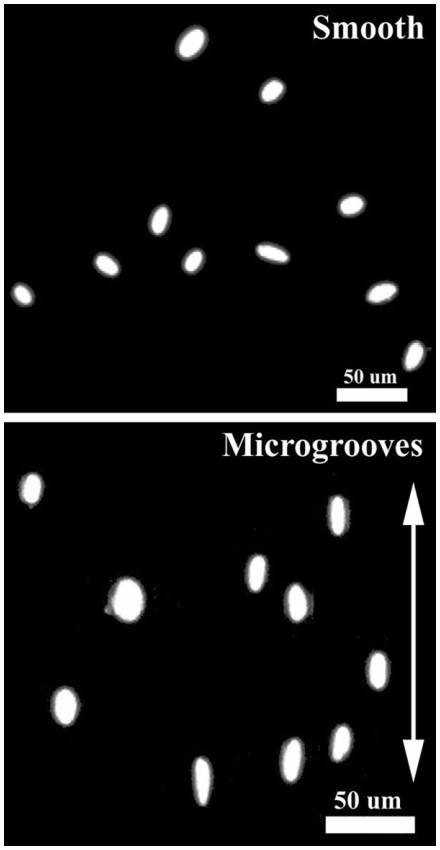

Figure 2.5. Osteoblast nucleus alignment on smooth control surface (top) and alignment on 7x7 μm patterned surface with a depth of 1 μm (bottom). Arrows represents the direction of patterned lines. Scale bars are equal to 50 μm

The nuclei on the microgrooved surface exhibit similar orientation corresponding to the microgroove direction while on the smooth control surface a random orientation can be observed. Aligned cells are those found to be within 10° of the reference angle determined by the mechanical grooves. Figure 2.6 presents the fraction of aligned cells for varying feature patterns and depths.

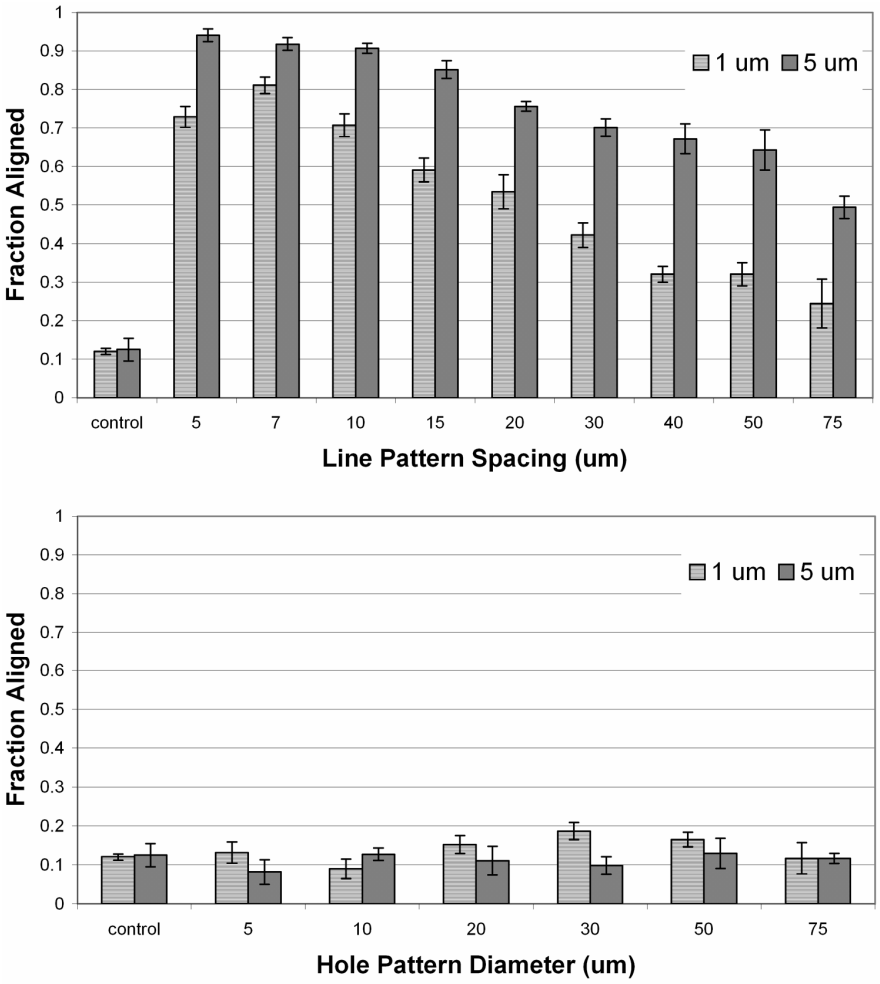

Figure 2.6. Alignment of cells on varying spacings of micropatterned lines for both 1 and 5 μm deep features. **Top** chart is for line patterns where the number is an AxA pattern spacing. **Bottom** chart is for hole patterns where the number is the hole diameter and 2A is the center-to-center distance. Error bars represent the standard deviation of each pattern type with n = 5.

For 1 μm deep features, the peak percentage of aligned cells was 81 ± 2.1% while for 5 μm the peak was 94 ± 1.6%. Pattern-dependent changes in alignment are observed on microgrooved patterns and not on the embossed hole patterns. The fraction of aligned cells for both depths decreases as feature size increases. This drop however is less pronounced in the 5 μm deep features as even for the 75 μm features the alignment in the deeper substrates is more than double that of the shallower samples. For the range of 5-75 μm microgrooves, two-way ANOVA revealed highly significant effects for both pattern

($p = 7.21\text{x}10^{-12}$) and depth ($p = 1.83\text{x}10^{-11}$). Furthermore, a significant interaction effect for micropattern and depth was detected ($p = 0.001$). No signifcant interactions were observed between microhole and alignment over the range of patterns and depths.

Cell proliferation, determined by BrdU incorporation, was selected as a complementary outcome marker to alignment to examine the effects of microtopography on higher order cell functions. Figure 2.7 shows the fraction of BrdU-positive cells on different patterns and depths. No significant differences were observed in the fraction of proliferating cells over the entire range of patterns and depths.

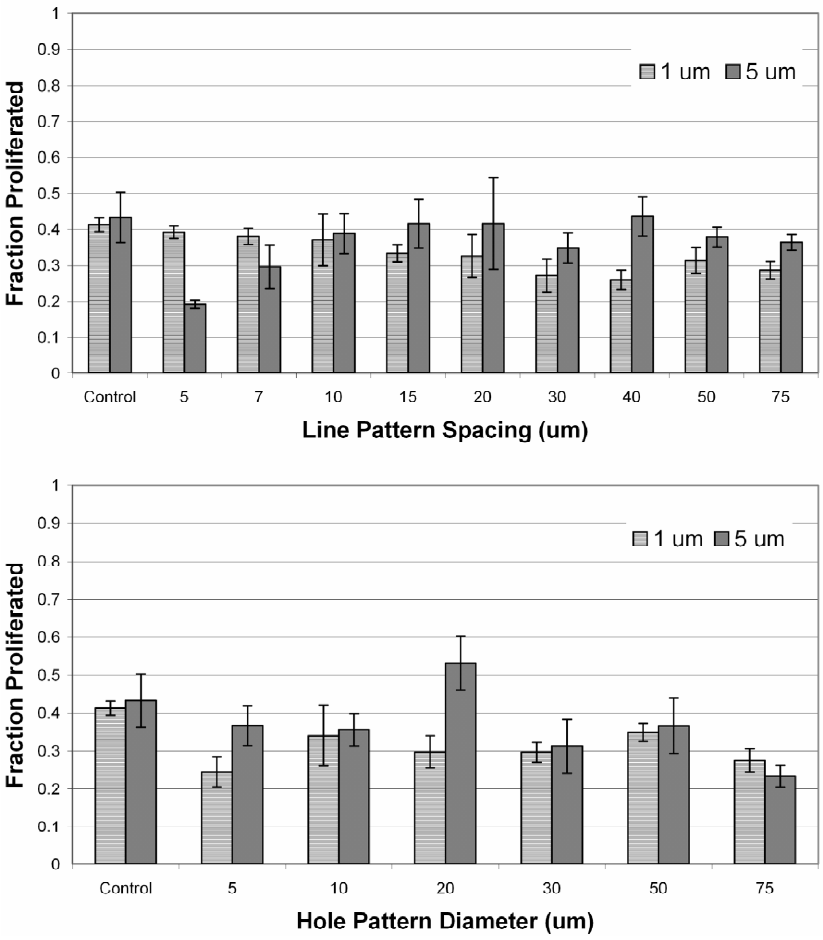

Figure 2.7. Proliferation on varying spacings of micropatterned lines for 1 and 5 μm deep features. **Top** chart is for line patterns where the number is an AxA pattern spacing. **Bottom** chart is for hole patterns where the number is the hole diameter and 2A is the center-to-center distance . Error bars represent the standard deviation of each pattern type with n = 4.

2.4 Discussion

This chapter demonstrates the use of a high-throughput chip to investigate cell response to micropatterns. This chip features 35 distinct patterns of grooves and holes with dimensions from 1-75 μm. 16 of these patterns were used in the work with sizes ranging from 5-75 μm. Figure 2.8 shows the transition between a 5x5 μm groove pattern and 5 μm diameter hole pattern on a 1 μm deep substrate.

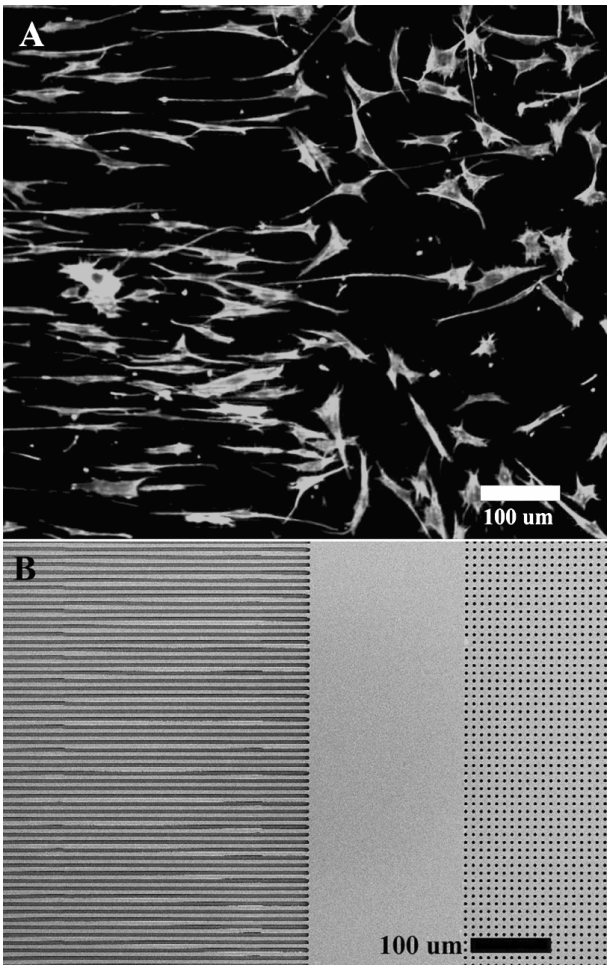

Figure 2.8. (**A**) IF image of actin filaments stained with rhodamine-phalloidin showing transition between 5x5 μm grooves (left) and 5 μm diameter holes (right) with a depth of 1 μm. (**B**) SEM image showing corresponding micropatterns to IF image. Both scale bars are equal to 100 μm.

This image shows the advantages of using a multiple pattern chip as cell differences can be immediately observed. Cells on the microgroove pattern show strong alignment when compared to the microholes that show no alignment. The SEM image is included to show the boundaries of the microfeatures. The number of patterns present on the chip allows for testing a large range of responses while decreasing the number of samples needed. This leads to less sample variation compared with experiments in which an individual sample is required for each pattern type.

Using the high-throughput chip it is shown that both feature spacing and depth have significant effects on cell alignment, but these surface parameters did not affect proliferation in our model cell system. Analysis shows that deep, narrow features have significantly higher cell alignment than that of shallow, wide features. This result is likely due to the location of cell bodies on the patterned substrates. For deep, narrow features the bulk of most cell bodies is centered within the microgrooves. Figure 2.9 shows cells within the microgrooved structure of a 5 μm deep feature as well as a cell body spanning multiple micropatterned grooves of a shallower feature.

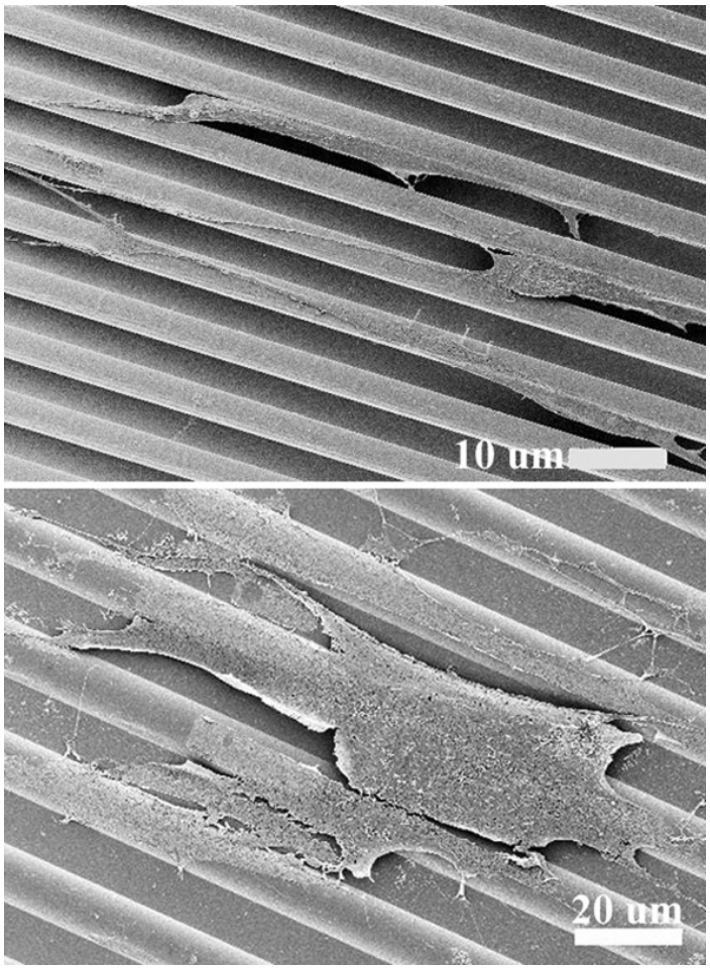

Figure 2.9. Comparison SEMs showing morphology differences of cells on substrates with different depths. Top image shows limited spreading of cells within a 5 μm deep grooves on a 5x5 μm pattern. Bottom image is of cell spreading over multiple pattern mesas on a 1 μm deep 10x10 μm pattern. Scale bar for top image is 10 μm and bottom image is 20 μm.

Cells on deeper grooves tend to span fewer grooves than those on shallower grooves. Cells on deeper grooves also appear to have the majority of the cell body within a microgroove. With less space to move around, cells on deep features may have less ability to spread. The lack of spreading could influence how the cell orients within the microgroove. The alignment results presented are similar to previous studies[1,7,9,26]. This work however presents the ability to test cell response to many different patterns on a single chip in an effort to lessen sample variability.

While the micropatterns heavily influenced cell alignment, they do not have a significant impact on cell proliferation. The fraction of cells that tested positive for BrdU incorporation remained nearly constant for all patterns and depths. The confinement of cells within a microgroove may be one reason why no significant differences in proliferation were observed. . Previous studies have shown that micropatterns have no effect upon proliferation[17,22] while others have shown a general decrease in proliferation from control when cells are cultured on micro and nanopatterns[21,27]. These studies however utilized different pattern types and fabrication methods which can impact the surface chemistry of the substrate. They also use different cell models than described in the present work. These methods may account for differences observed.

2.5 Conclusion

This chapter reports the use of a high-throughput chip design to study the impact that mciropattern spacing, type, and depth has upon cell function. A single chip that featured 35 different micropatterns was fabricated using hot embossing and used in parallel to limit sample variability. Each chip had a well defined, consistent surface chemistry that further reduced sample variability. Results for the influence of micropatterns on cell alignment and proliferation were consistent with previous studies. While strong interactions were determined for cellular alignment to microfeatures, interactions between samples and cell proliferation were not significant. This work however makes use of a single chip design that allows for less variability amongst samples as well as a quicker fabrication time as fewer samples are required. This technique allows for a wider range of surface interactions to be tested at one time. A

greater understanding of how cells respond to patterned substrates will assist with the development of many biotechnologies.

2.6 References

1. Charest JL, Bryant LE, Garcia AJ, King WP. Hot embossing for micropatterned cell substrates. Biomaterials 2004;25(19):4767-4775.

2. Curtis A, Wilkinson C. Topographical control of cells. Biomaterials 1997;18(24):1573-1583.

3. Flemming RG, Murphy CJ, Abrams GA, Goodman SL, Nealey PF. Effects of synthetic micro- and nano-structured surfaces on cell behavior. Biomaterials 1999;20:573–588.

4. Schwartz Z, Boyan BD. Underlying Mechanisms at the Bone-Biomaterial Interface. Journal of Cellular Biochemistry 1994;56(3):340-347.

5. Clark P, Connolly P, Curtis ASG, Dow JAT, Wilkinson CDW. Topographical Control of Cell Behavior .1. Simple Step Cues. Development 1987;99(3):439-448.

6. Chou SY, Krauss PR, Renstrom PJ. Imprint lithography with 25-nanometer resolution. Science 1996;272(5258):85-87.

7. Clark P, Connolly P, Curtis ASG, Dow JAT, Wilkinson CDW. Topographical Control of Cell Behavior .2. Multiple Grooved Substrata. Development 1990;108(4):635-644.

8. Mata A, Boehm C, Fleischman AJ, Muschler G, Roy S. Analysis of connective tissue progenitor cell behavior on polydimethylsiloxane smooth and channel micro-textures. Biomedical Microdevices 2002;4(4):267-275.

9. Oakley C, Brunette DM. The Sequence of Alignment of Microtubules, Focal Contacts and Actin-Filaments in Fibroblasts Spreading on Smooth and Grooved Titanium Substrata. Journal of Cell Science 1993;106:343-354.

10. Parker J, Walboomers XF, Von den Hoff JW, Maltha JC, Jansen JA. Soft tissue response to microtextured silicone and poly-L-lactic acid implants: fibronectin pre-coating vs. radio-frequency glow discharge treatment. Biomaterials 2002;23(17):3545-3553.

11. Rovensky YA, Slavnaja IL, Vasiliev JM. Behaviour of Fibroblast-Like Cells on Grooved Surfaces. Experimental Cell Research 1971;65(1):193-&.

12. Schmidt JA, Vonrecum AF. Surface Characterization of Microtextured Silicone. Biomaterials 1992;13(10):675-681.

13. Snyder JD, Desai TA. Microscale three-dimensional polymeric platforms for in vitro cell culture systems. Journal of Biomaterials Science-Polymer Edition 2001;12(8):921-932.

14. van Kooten TG, von Recum AF. Cell adhesion to textured silicone surfaces: The influence of time of adhesion and texture on focal contact and fibronectin fibril formation. Tissue Engineering 1999;5(3):223-240.

15. van Kooten TG, Whitesides JF, von Recum AF. Influence of silicone (PDMS) surface texture on human skin fibroblast proliferation as determined by cell cycle analysis. Journal of Biomedical Materials Research 1998;43(1):1-14.

16. Walboomers XF, Croes HJE, Ginsel LA, Jansen JA. Contact guidance of rat fibroblasts on various implant materials. Journal of Biomedical Materials Research 1999;47(2):204-212.

17. Wang JHC, Grood ES, Florer J, Wenstrup R. Alignment and proliferation of MC3T3-E1 osteoblasts in microgrooved silicone substrata subjected to cyclic stretching. Journal of Biomechanics 2000;33(6):729-735.

18. Chou SY, Krauss PR. Imprint lithography with sub-10 nm feature size and high throughput. Microelectronic Engineering 1997;35(1-4):237-240.

19. Charest JL, Eliason MT, Garcia AJ, King WP. Combined microscale mechanical topography and chemical patterns on polymer cell culture substrates. Biomaterials 2006;27(11):2487-2494.

20. Charest JL, Eliason MT, Garcia AJ, King WP, Talin AA, Simmons BA. Polymer cell culture substrates with combined nanotopographical patterns and micropatterned chemical domains. Journal of Vacuum Science & Technology B 2005;23(6):3011-3014.

21. Thakar RG, Ho F, Huang NF, Liepmann D, Li S. Regulation of vascular smooth muscle cells by micropatterning. Biochemical and Biophysical Research Communications 2003;307(4):883-890.

22. Wan YQ, Wang Y, Liu ZM, Qu X, Han BX, Bei JZ, Wang SG. Adhesion and proliferation of OCT-1 osteoblast-like cells on micro- and nano-scale topography structured pply(L-lactide). Biomaterials 2005;26(21):4453-4459.

23. Keselowsky BG, Collard DM, Garcia AJ. Surface chemistry modulates fibronectin conformation and directs integrin binding and specificity to control cell adhesion. Journal of Biomedical Materials Research Part A 2003;66A(2):247-259.

24. Keselowsky BG, Collard DM, Garcia AJ. Integrin binding specificity regulates biomaterial surface chemistry effects on cell differentiation. Proceedings of the National Academy of Sciences of the United States of America 2005;102(17):5953-5957.

25. Lan MA, Gersbach CA, Michael KE, Keselowsky BG, Garcia AJ. Myoblast proliferation and differentiation on fibronectin-coated self assembled monolayers presenting different surface chemistries. Biomaterials 2005;26(22):4523-4531.

26. Teixeira AI, Abrams GA, Bertics PJ, Murphy CJ, Nealey PF. Epithelial contact guidance on well-defined micro- and nanostructured substrates. Journal of Cell Science 2003;116(10):1881-1892.

27. Yim EKF, Reano RM, Pang SW, Yee AF, Chen CS, Leong KW. Nanopattern-induced changes in morphology and motility of smooth muscle cells. Biomaterials 2005;26(26):5405-5413.

CHAPTER 3

POLYMER CELL CULTURE SUBSTRATES WITH MICROPATTERNED CARBON NANOTUBES

This chapter presents study of the interactions between cells and micropatterned carbon nanotubes on a polymer cell culture substrate. The polymer substrates with patterned carbon nanotubes were fabricated using an imprint process, whereby the nanotubes were pressed into a polymer layer at high temperature. The patterned substrates featured 28 different nanotube patterns of microscale lanes and circles, where the feature sizes ranged from 9 to 76 μm. Osteoblast-like cells were seeded on the substrates and cell alignment was quantified via fluorescent and electron microscopy. Many patterns were fabricated on each polymer substrate, allowing 28 different experiments on each cell culture substrate, which tested over 10,000 cells. The cell response to the patterned nanotubes showed a maximum alignment to the microlane patterns of 55 ± 6 % although no significant alignment to microcircle patterns. This work enables the study of cell response to a wider range of patterns featuring both the micro and nano length scales.

3.1 Introduction

Cells interact with extracellular matrix (ECM) components spanning the millimeter, micrometer, and nanometer length scales. The successful implementation of many emerging biotechnologies may require controlled presentation of synthetic

microscale and nanoscale features to simulate the *in vivo* environment. This chapter reports on the fabrication of cell culture substrates having embedded carbon nanotubes, where the resulting substrates have combinations of microscale and nanoscale topographical features.

Adherent cells exhibit complex interactions with nearby surfaces. Many cell functions such as alignment, proliferation and differentiation are sensitive to the surroundings[1-3]. It is now well known that cells respond to microscale and nanoscale topographical features that exist on a cell culture substrate[1,2,4-11]. These studies generally employ cell substrates made of glass, silicon and polymers. Of these materials, polymers are an attractive material due to their ease of use and low cost. Cell culture substrates formed from materials like silicon require significant capital equipment in order to form microtopographies. The fabrication of nanometer-scale features using traditional silicon machining can be substantially more complex than the fabrication of micrometer-scale features. Polymer materials offer an easier route to fabrication of complex substrates having micrometer and nanometer-scale features.

Widespread interest in the properties of nanomaterials has motivated investigations of cell substrates based on nanofiber constructs[12-18]. These constructs are generally substrates with a full coverage of nanofibrous material such as carbon nanotubes. These systems also are generally grown on silicon substrates, making them less attractive for *in vivo* systems compared to polymers. Furthermore, while these nanopatterned surfaces are interesting model systems, they generally do not combine patterns of multiple length scales. While a few published reports have described cell culture substrates having patterns with multiple length scales[18-20], much work remains

in understanding of cell responses to substrates having topographical patterns with multiple length scales. To date, no paper has been published on cellular response to patterns of carbon nanotubes on polymer substrates. This chapter presents a technique to fabricate polymer cell culture substrates having micropatterns of embedded carbon nanotubes, and analyzes the alignment of osteoblast-like cells to these patterns.

3.2 Materials and Methods

Hot embossing was used to fabricate polymer cell culture substrates having micropatterns of carbon nanotubes[21-24]. The alignment of MC3T3-E1 osteoblast-like cells was analyzed on microtopographies of lanes and circles formed from pressed carbon nanotubes. Microlane and circle features ranged from 9 to 75 μm in width. Fluorescence and scanning electron microscopy were used to analyze cell alignment to the patterns of carbon nanotubes.

3.2.1 Substrate Fabrication

Patterned carbon nanotube masters were combined with a hot embossing imprint lithography process to produce the polymer cell substrates. Figure 3.1 shows a schematic of the carbon nanotube hot embossing process.

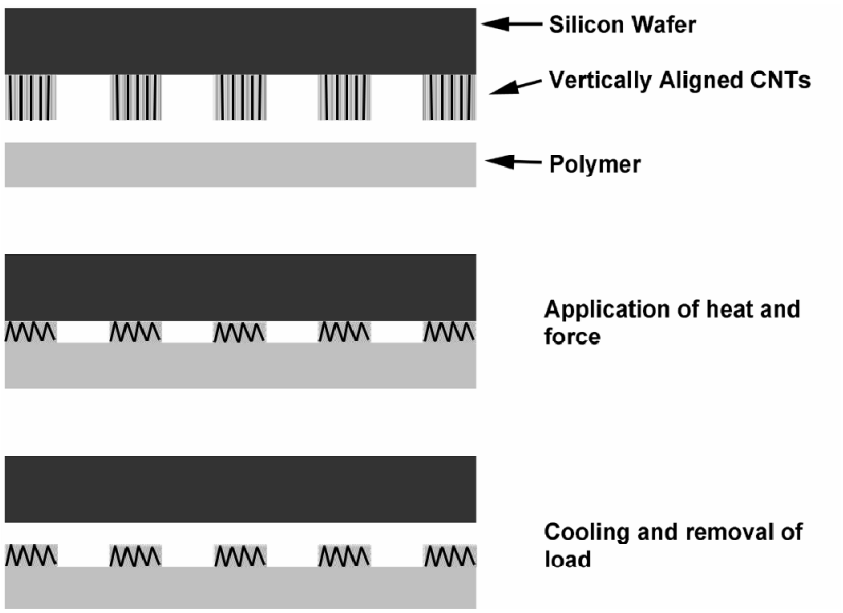

Figure 3.1. Schematic of carbon nanotube embossing process used to fabricate polymer cell culture substrates. Vertically aligned CNTs are grown on a Si wafer surface and brought into contact with a polymer substrate under heat and force. Once cool, the master is removed leaving the polymer with embedded CNTs.

The carbon nanotubes were synthesized on a silicon substrate having a thin layer of silicon dioxide and layer of micropatterned iron formed using standard microfabrication techniques. The micropatterns consisted of lines and circles with sizes ranging from 1-75 μm on each substrate. The masters also had nonpatterned, flat regions, or regions fully filled with nanotubes, to be used for control experiments. To synthesize the carbon nanotubes, samples were placed in a furnace and heated to 700°C for 10 minutes of argon flow at 1000 sccm, then at 2 minutes ethylene with at 700 sccm. The nanotubes formed were vertically-aligned multi-wall nanotubes (MWNT) with an approximate diameter of 25 nm and height 4 μm. Figure 3.2 shows the nanotubes grown on the silicon masters.

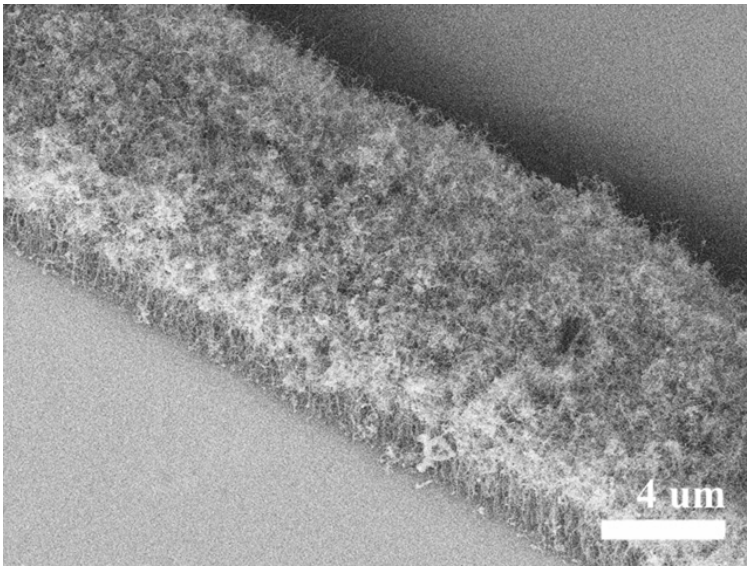

Figure 3.2. Scanning electron micrographs of vertically aligned CNTs grown on a Si wafer. Nanotube height is approximately 4 μm.

After CNT synthesis, hot embossing was used to transfer nanotube patterns onto a polymer layer. Previously, hot embossing has been used to replicate microfabricated features into polymer layers[5] but has also been combined with CNTs to study flexible electronics[21,22]. The master template was placed in contact with a smooth 0.5 mm-thick polycarbonate (PC) substrate, heated to 143°C, and embossed into the polymer with a pressure of 6.7 MPa for 5 minutes. After cooling to room temperature, the load was released and the master removed from the substrate. After the embossing step, samples were characterized using optical and scanning electron microscopy.

3.2.2 Cell Culture

The fabricated substrates were prepared for cell growth as follows. The nanotube embossed samples were coated with 100Å Ti and 200Å Au using an electron-beam evaporator. Samples were immersed in hexadecanethiol (HDT) and dried under nitrogen

stream to create uniform surface chemistry[25,26]. Next, samples were sterilized in 95% ethanol, rinsed in PBS and coated with fibronectin (20 μm/mL) for 30 minutes. After 1-hour of incubation in 1% heat denatured bovine serum albumin (BSA) at 37°C and 5% CO_2, MC3T3-E1 osteoblast-like cells were seeded at a density of 50 cells/mm^2. Cells were cultured in α-minimal essential medium with 10% serum and 1% penicillin-streptomycin.

Samples were then prepared for analysis of cell alignment. After 18 hours in culture, cells were permeablized in 0.5% Triton X-100 cytoskeleton buffer (50 mM NaCl, 150 nM sucrose, 3mM $MgCl_2$, 50 mM tris(hydroxymethyl), 20 μg/mL aprotinin, and 1 μg/mL with pH of 6.8) for 5 minutes and fixed with 3.7% formaldehyde in PBS for 2 min. Samples were then incubated for 1-hour in BSA. Next, samples were incubated in a primary antibody against fibronectin for 1-hour, rinsed twice in PBS, incubated in BSA for 10 minutes and followed with two more PBS rinses. They were then incubated in secondary fluorochrome labeled anti-IgG, rhodamine-phalloidin and Hoechst DNA stain for 1 hour, rinsed as before and mounted on glass slides. Samples were examined using a fluorescent microscope and processed using image processing software.

3.2.3 Analysis

Cellular alignment was determined by fitting an ellipse to cell nuclei, as this has previously been shown to be appropriate for measuring overall cell alignment[5]. The angle of the major axis of the ellipse was normalized to a reference angle determined by the angle of patterned nanotube features, resulting in an angle measurement from 0-90° with angles less than or equal to 10° considered aligned. For SEM preparation, samples were rinsed twice in PBS and then fixed in 2.5% glutaraldehyde in PBS for 30 minutes at

4°C. Following two more rinses in PBS, samples were dehydrated in increasing concentrations of ethanol (70%, 90% and 100%) for 30 minutes each. Samples were then soaked twice in hexamethyldisilazane (HMDS) for 30 minutes each. Samples were then left to dry overnight in a desiccator before in SEM.

3.2.4 Statistics

Experiments for cell alignment were conducted independently with a minimum of n = 4. Results are reported as mean ± standard error of the mean. Interactions were tested using an ANOVA with pattern as the fixed variable using SYSTAT 8.0. *P*-values less than 0.05 were considered significant.

3.3 Results and Discussion

The fabricated polymer-nanotube substrates were characterized using SEM and optical microscopy. Figure 3.3 shows the polymer substrate having the micropatterned nanotubes, where the nanotube height was 4 μm.

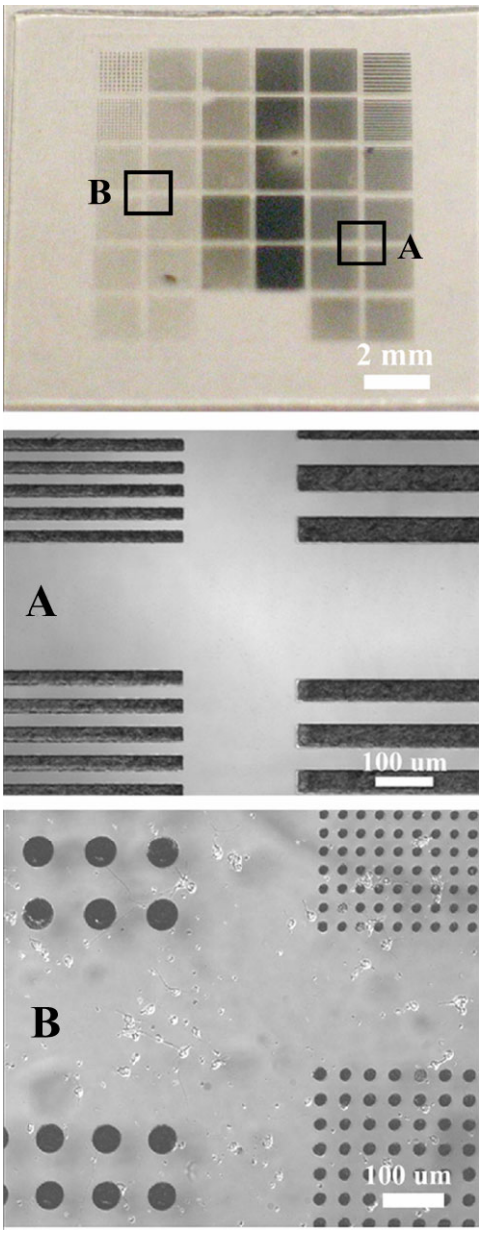

Figure 3.3. Picture showing high throughput chip layout. Each chip contains multiple patterns for high throughput analysis. Expanded images are optical micrographs showing CNT line patterns (A) and CNT dot patterns (B) in close proximity to each other.

Good replication was achieved of the original patterns, although the embossed features are 1 to 2 μm wider than the master patterns, due to the height of the nanotubes. The patterns examined in this work had spacing of 9, 11.5, 16, 21, 31, 41, 51, and 76 μm. It is well known that surface topography can influence cellular alignment[1,2,5,7], and so

the height of the nanotubes on the polymer substrates was analyzed. Figure 3.4 shows a typical profile of the embossed nanotube features, where the nanotubes are nearly flush with the nonpatterned polymer surface. Overall it was observed that the embossed features had a negligible height compared to the polymer substrate.

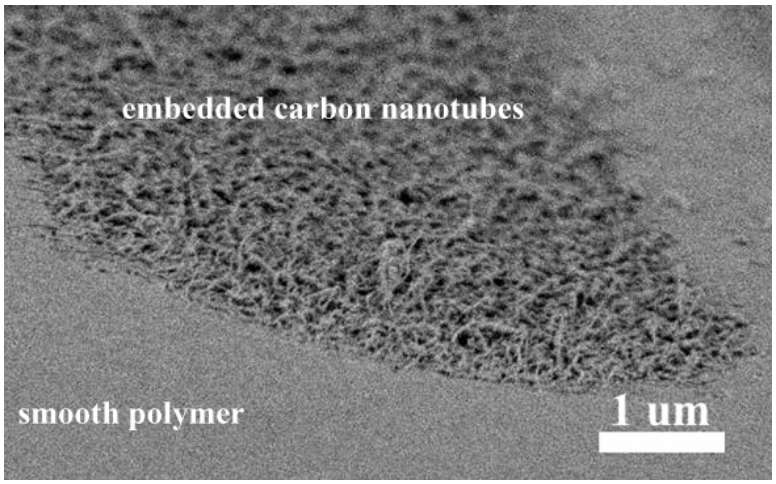

Figure 3.4. Scanning electron micrograph showing profile of embedded CNT features in the smooth polymer substrate. Scale bar is equal to 1 μm.

The cells were characterized on the micropatterned nanotubes using SEM and fluorescence microscopy. Cell alignment was determined by the angle of the cell nucleus with respect to the patterned features, and confirmed by observation of the cell body. Nucleus alignment was determined by fitting an ellipse to the nucleus and measuring the angle to the major axis. Figure 3.5 shows the fraction of aligned cells for each of the pattern types and spacings.

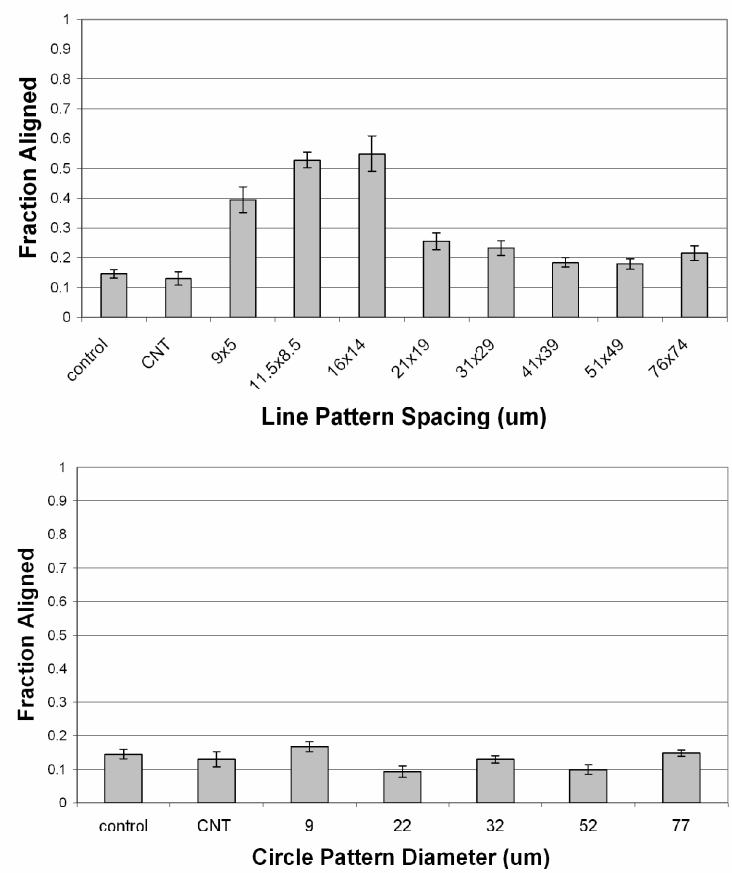

Figure 3.5. Summary of cell response to the CNT patterns. The top graph shows alignment to micropatterned lines and bottom is alignment to micropatterned circles. "Control" refers to nanotube free areas while "CNT" refers to a carbon nanotube filled zone. Error bars indicate the standard error of the samples.

The cells exhibited peak alignment to the patterned lines of 55 ± 6 % at feature spacings in the range 10 - 15 μm. The cells exhibited no clear alignment on the circular nanotube patterns. Control samples, which had either no nanotubes or complete fill of the nanotubes, were also taken for reference. Using an ANOVA test, a significant cell interaction is seen for the line pattern ($p = 9.13 \times 10^{-12}$) but no significant interaction for the circles. Cell bodies were analyzed to confirm the alignment determined from the cell nucleus. By staining the actin cytoskeleton of the cell it was possible to observe the orientation of the cell body, which was done to confirm that the cell body was oriented in

the direction of the cell nucleus. Figure 3.6 shows images of cell bodies on a flat control surface and a nanotube pattern of 15 μm lines. The cells are randomly aligned on the smooth surface, but strongly oriented in the direction of the nanotube lines.

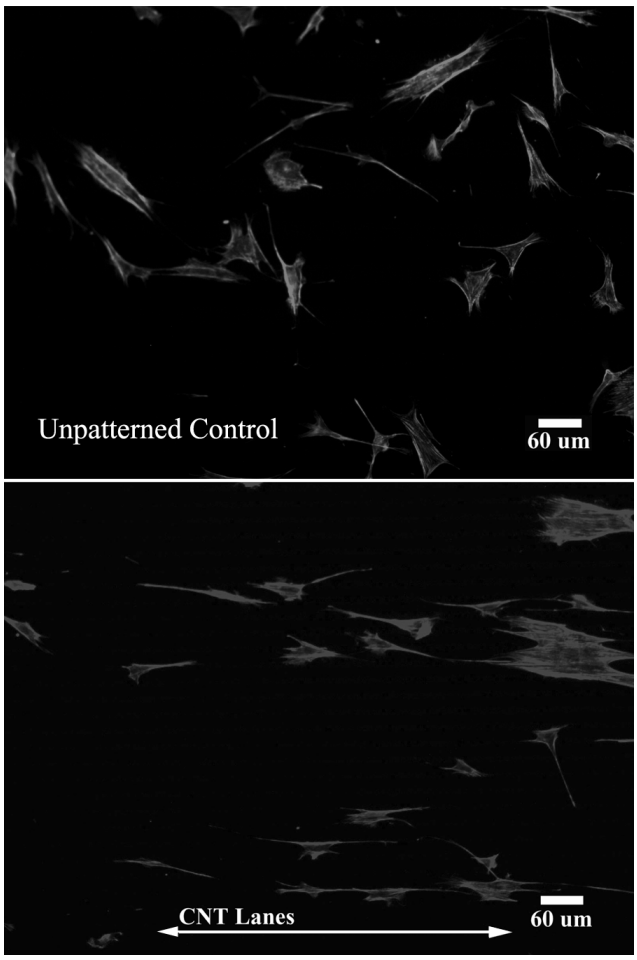

Figure 3.6. Flouresence microscopy images showing (top) randomly aligned cell bodies on a flat control surface and (bottom) aligned cell bodies to a 16 x 14 μm CNT. Arrows denote the direction of the patterned nanotube lines.

Previous studies of cell response to substrates having nanometer-scale features has been mostly limited to substrates having only nanoscale topography or roughness[6-9,11,27-29], and in general are few studies that investigate micropatterns of nanostructures. Some research has investigated nanometer-scale topographical patterns

combined with micron-scale chemical domains[20]. There are however few published reports that investigate the combination of both micro and nanoscale mechanical topographies. In the present study, hot embossing is used to manufacture fabricate micron-scale patterns of carbon nanotubes into polymer cell substrates. The resulting substrates have 28 different pattern types consisting of nanoscale patterns over well defined micron-scale features. Significant interactions were observed between pattern type and cell alignment. Since the substrate exhibits little vertical topography, the cell alignment is most likely due to interactions with the nanometer-scale roughness presented by the patterned nanotubes. Figure 3.7 shows a cell on a flat control surface, where a few cell extensions can be seen. In comparison, Figure 3.8 shows a cell on a patterned carbon nanotube surface, where the cell has many cell extensions on the nanotube patterns.

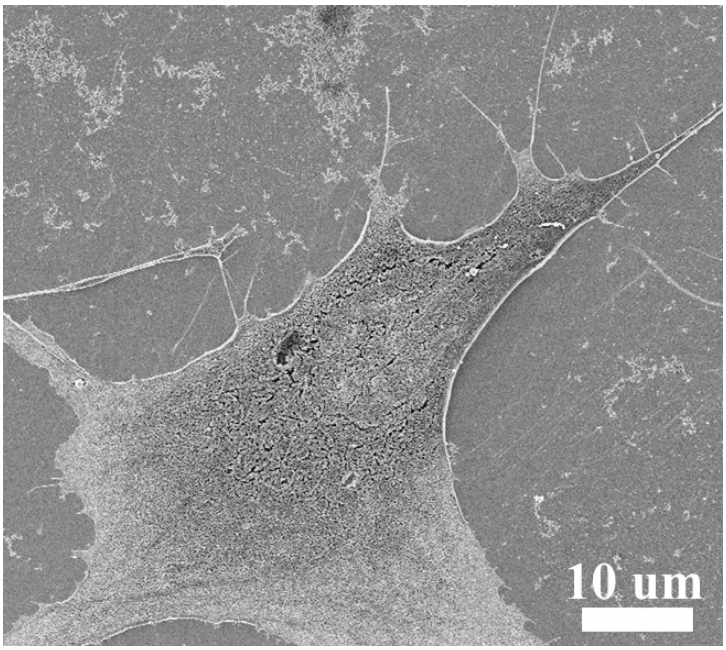

Figure 3.7. Scanning electron micrograph of cell on flat polymer substrate. Cell has low number of cell extensions interacting with the flat surface. Scale bar equal to 10 um.

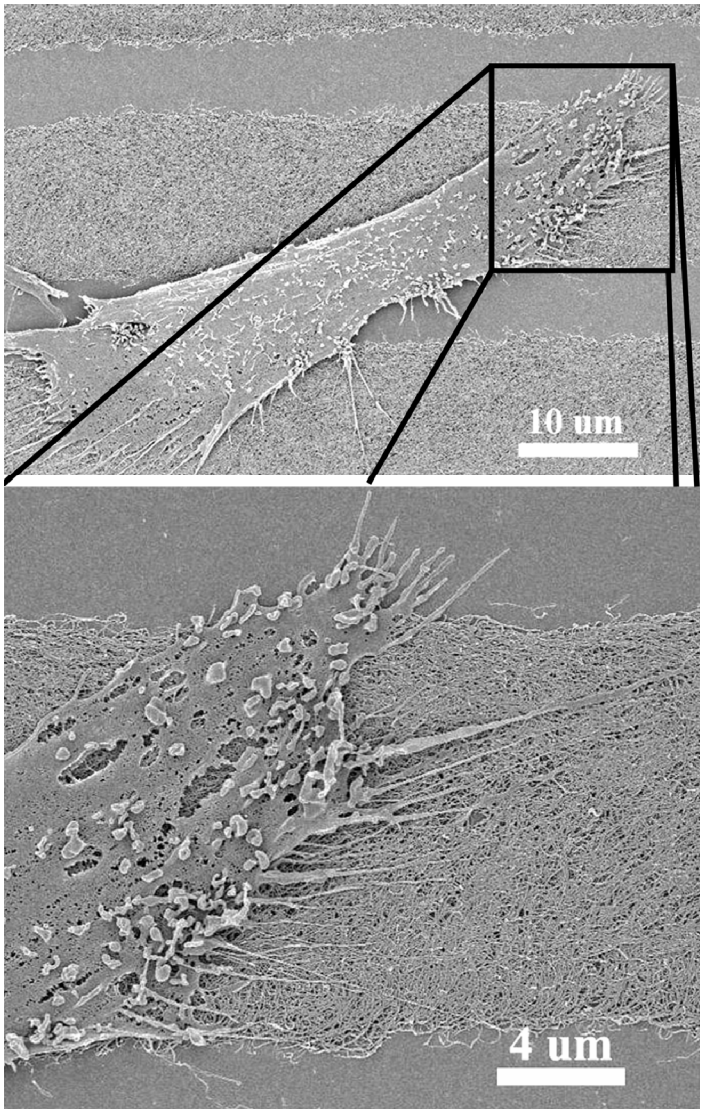

Figure 3.8. Scanning electron micrographs showing a single cell on embossed CNT lanes. Expanded image shows the increased interactions between cell extensions and CNT patterns. Top image has a scale bar of 10 μm and the bottom image has a scale bar of 4 μm.

The presence of many cell extensions on the patterns of nanotubes is consistent with the observed cell alignment, as cell extensions are responsible for cell movement and surface sensing. The increase of extensions could be due to a preferential adhesion to the nanopatterns over flat surfaces, which has been observed in other studies[18]. Other

studies have shown an increase in small adhesive point contacts to nanotubes[12] as well as morphological changes that can affect cell function[17].

For micro- or nano-fabricated cell substrates to have biomedical application, a major challenge will be biocompatibility. While long-term biocompatibility of carbon materials is still being researched[30-34], polymer substrates may offer advantages over silicon substrates.

3.4 Conclusion

This chapter reports the fabrication of polymer cell culture substrates having patterns of embedded carbon nanotubes, and the alignment of osteoblast cells to those surfaces. The experimental platform was a single chip having 28 different patterns of embedded carbon nanotubes, where a consistent surface chemistry was achieved on each sample to limit sample variability. Significant cell alignment was observed on the nanotube line features, while no interaction was observed between the nanotube circles and cell alignment. This work shows the potential to use carbon nanotubes to present combined microscale and nanoscale patterns on polymer cell culture substrates.

3.5 References

1. Clark P, Connolly P, Curtis ASG, Dow JAT, Wilkinson CDW. Topographical Control of Cell Behavior .1. Simple Step Cues. Development 1987;99(3):439-448.

2. Clark P, Connolly P, Curtis ASG, Dow JAT, Wilkinson CDW. Topographical Control of Cell Behavior .2. Multiple Grooved Substrata. Development 1990;108(4):635-644.

3. Curtis A, Wilkinson C. Topographical control of cells. Biomaterials 1997;18(24):1573-1583.
4. Bhatia SN, Chen CS. Tissue Engineering at the Micro-Scale Biomedical Microdevices 1999;2(2):131-144

5. Charest JL, Bryant LE, Garcia AJ, King WP. Hot embossing for micropatterned cell substrates. Biomaterials 2004;25(19):4767-4775.

6. Dalby MJ, Gadegaard N, Riehle MO, Wilkinson CDW, Curtis ASG. Investigating filopodia sensing using arrays of defined nano-pits down to 35 nm diameter in size. International Journal of Biochemistry & Cell Biology 2004;36(10):2005-2015.

7. Flemming RG, Murphy CJ, Abrams GA, Goodman SL, Nealey PF. Effects of synthetic micro- and nano-structured surfaces on cell behavior. Biomaterials 1999;20:573–588.

8. He W, Gonsalves KE, Batina N, Poker DB, Alexander E, Hudson M. Micro/nanomachining of polymer surface for promoting Osteoblast cell adhesion. Biomedical Microdevices 2003;5(2):101-108.

9. Teixeira AI, Abrams GA, Bertics PJ, Murphy CJ, Nealey PF. Epithelial contact guidance on well-defined micro- and nanostructured substrates. Journal of Cell Science 2003;116(10):1881-1892.

10. Wan YQ, Wang Y, Liu ZM, Qu X, Han BX, Bei JZ, Wang SG. Adhesion and proliferation of OCT-1 osteoblast-like cells on micro- and nano-scale topography structured pply(L-lactide). Biomaterials 2005;26(21):4453-4459.

11. Wilkinson CDW, Curtis ASG, Crossan J. Nanofabrication in cellular engineering. Journal of Vacuum Science & Technology B 1998;16(6):3132-3136.

12. George JH, Shaffer MS, Stevens MM. Investigating the cellular response to nanofibrous materials by use of a multi-walled carbon nanotube model. Journal of Experimental Nanoscience, 2006;in press.

13. Ma ZW, Kotaki M, Inai R, Ramakrishna S. Potential of nanofiber matrix as tissue-engineering scaffolds. Tissue Engineering 2005;11(1-2):101-109.

14. Smith LA, Ma PX. Nano-fibrous scaffolds for tissue engineering. Colloids and Surfaces B-Biointerfaces 2004;39(3):125-131.

15. Stevens MM, George JH. Exploring and engineering the cell surface interface. Science 2005;310(5751):1135-1138.

16. Venugopal J, Ramakrishna S. Applications of polymer nanofibers in biomedicine and biotechnology. Applied Biochemistry and Biotechnology 2005;125(3):147-157.

17. Zanello LP, Zhao B, Hu H, Haddon RC. Bone cell proliferation on carbon nanotubes. Nano Letters 2006;6(3):562-567.

18. Zhang X, Prasad S, Niyogi S, Morgan A, Ozkan M, Ozkan CS. Guided neurite growth on patterned carbon nanotubes. Sensors and Actuators B-Chemical 2005;106(2):843-850.

19. Charest JL, Eliason MT, Garcia AJ, King WP. Combined microscale mechanical topography and chemical patterns on polymer cell culture substrates. Biomaterials 2006;27(11):2487-2494.

20. Charest JL, Eliason MT, Garcia AJ, King WP, Talin AA, Simmons BA. Polymer cell culture substrates with combined nanotopographical patterns and micropatterned chemical domains. Journal of Vacuum Science & Technology B 2005;23(6):3011-3014.

21. Allen A, Cannon A, Lee J, King WP, Graham S. Flexible microdevices based on carbon nanotubes. Journal of Micromechanics and Microengineering 2006;16(12):2722-2729.

22. Allen AC, Sunden E, Cannon A, Graham S, King W. Nanomaterial transfer using hot embossing for flexible electronic devices. Applied Physics Letters 2006;88(8):083112.

23. Cannon AH, Allen AC, Graham S, King WP. Molding ceramic microstructures on flat and curved surfaces with and without embedded carbon nanotubes. JOURNAL OF MICROMECHANICS AND MICROENGINEERING 2006;16(12):2554–2563.

24. Sunden E, Moon JK, Wong CP, King WP, Graham S. Microwave assisted patterning of vertically aligned carbon nanotubes onto polymer substrates. Journal of Vacuum Science & Technology B 2006;24(4):1947-1950.

25. Keselowsky BG, Collard DM, Garcia AJ. Surface chemistry modulates fibronectin conformation and directs integrin binding and specificity to control cell adhesion. Journal of Biomedical Materials Research Part A 2003;66A(2):247-259.

26. Keselowsky BG, Collard DM, Garcia AJ. Integrin binding specificity regulates biomaterial surface chemistry effects on cell differentiation. Proceedings of the National Academy of Sciences of the United States of America 2005;102(17):5953-5957.

27. Dalby MJ, Riehle MO, Johnstone H, Affrossman S, Curtis ASG. Investigating the limits of filopodial sensing: a brief report using SEM to image the interaction between 10 nm high nano-topography and fibroblast filopodia. Cell Biology International 2004;28(3):229-236.

28. Price RL, Ellison K, Haberstroh KM, Webster TJ. Nanometer surface roughness increases select osteoblast adhesion on carbon nanofiber compacts. Journal of Biomedical Materials Research Part A 2004;70A(1):129-138.

29. Yim EKF, Reano RM, Pang SW, Yee AF, Chen CS, Leong KW. Nanopattern-induced changes in morphology and motility of smooth muscle cells. Biomaterials 2005;26(26):5405-5413.

30. Magrez A, Kasas S, Salicio V, Pasquier N, Seo JW, Celio M, Catsicas S, Schwaller B, Forro L. Cellular toxicity of carbon-based nanomaterials. Nano Letters 2006;6(6):1121-1125.

31. Manna SK, Sarkar S, Barr J, Wise K, Barrera EV, Jejelowo O, Rice-Ficht AC, Ramesh GT. Single-walled carbon nanotube induces oxidative stress and activates nuclear transcription factor-kappa B in human keratinocytes. Nano Letters 2005;5(9):1676-1684.
32. Monteiro-Riviere NA, Nemanich RJ, Inman AO, Wang YYY, Riviere JE. Multi-walled carbon nanotube interactions with human epidermal keratinocytes. Toxicology Letters 2005;155(3):377-384.
33. Shvedova AA, Castranova V, Kisin ER, Schwegler-Berry D, Murray AR, Gandelsman VZ, Maynard A, Baron P. Exposure to carbon nanotube material: Assessment of nanotube cytotoxicity using human keratinocyte cells. Journal of Toxicology and Environmental Health-Part A 2003;66(20):1909-1926.
34. Shvedova AA, Kisin ER, Mercer R, Murray AR, Johnson VJ, Potapovich AI, Tyurina YY, Gorelik O, Arepalli S, Schwegler-Berry D and others. Unusual inflammatory and fibrogenic pulmonary responses to single-walled carbon nanotubes in mice. American Journal of Physiology-Lung Cellular and Molecular Physiology 2005;289(5):L698-L708.

CHAPTER 4

NANOIMPRINT FABRICATION OF POLYMER CELL SUBSTRATES HAVING COMBINED MICROMETER-SCALE AND NANOMETER-SCALE TOPOGRAPHY

This chapter reports the fabrication of polymer cell culture substrates having combined micrometer-scale and nanometer-scale topography. The substrates were fabricated using two embossing steps, where the large features were formed in the first emboss and then the smaller features were formed in the second. The first emboss produced grooves of width either 2 or 10 μm, while the second emboss produced grooves 50 nm wide on a 150 nm pitch. The 50 nm grooves were either parallel to or perpendicular to the microgrooves. Osteoblast-like cells were seeded onto the substrates and cell alignment analyzed using fluorescent and scanning electron microscopy. There was a significant decrease in alignment for microfeatures with perpendicular nanofeatures compared to those with parallel nanofeatures. This research enables cell response to be examined to complex combinations of micron-scale and nano-scale topography.

4.1 Introduction

The successful implementation of many emerging biotechnologies requires effort to mimic conditions found *in vivo*. One such condition is to approximate cell interactions with extracellular matrix (ECM) components, which have mechanical and chemical features that span the millimeter, micrometer, and nanometer length scales[1,2].

Synthetic cell culture substrates must therefore be able to present to adherent cells topographical features having multiple length scales. This chapter reports the fabrication of polymer cell culture substrates having both micrometer scale and nanometer scale topography, and analyzes the response of osteoblast-like cells to these substrates.

The fate of adherent cells depends upon the surfaces to which they are attached. Cell alignment, proliferation, and differentiation all depend upon surface characteristics[3-5]. Many studies have examined the cell response to surfaces having patterned features[1,6-13]. In general, the substrates used in these studies are fabricated from silicon, glass, or polymers. Of these materials, polymers offer the lowest cost and ease of use for fabrication of substrates with complex patterns over multiple length scales. While traditional microfabrication processes can easily be used to make micron-scale features, nanometer-scale features are somewhat more difficult to produce in silicon or glass. Electron beam lithography can be used for nanopatterning but is expensive and time consuming, particularly if many samples are required. Molding and other replication technologies can be used to fabricate either micron-scale or nanometer-scale features into polymer substrates with high throughput and low cost compared to electron-beam lithography[7,14,15]. Polymer cell substrates are also attractive as polymer properties are tunable to the desired application and many can be used *in vivo*[16].

While many studies have examined cell response to micrometer-scale features and nanometer-scale features, very few have investigated combinations of these length scales. Studies that explore combinations of topographical length scales have shown cell response to patterned carbon nanotubes[17] and the addition of chemical microdomains to nanogrooves substrates[15]. Embossing is one of the preferred routes to achieving

multiple length scales[18,19], however the cell response to such patterns has not been reported. This chapter uses nanoimprint lithography to fabricate polymer cell substrates having both micron-scale and nanometer-scale features and analyzes the cell response to these complex patterns.

4.2 Materials and Methods

4.2.1 Substrate Fabrication

Multiple hot embossing steps[7] were used to form the cell substrate surface topography to have both micron-scale and nanometer-scale surface features[18,19]. Figure 4.1 shows a schematic of hot embossing in which a template is pressed into a polymer at elevated temperature.

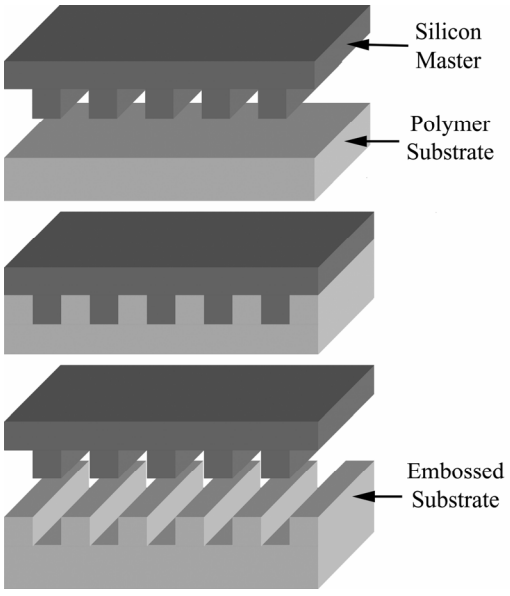

Figure 4.1. Schematic of the hot embossing process. In this process a silicon micromachined master is brought into contact with a polymer layer under heat and force. After the desired embossing time, the mold is cooled and removed leaving replicate features in the polymer substrate.

The master templates used to form the micron-scale features were fabricated from silicon using standard photolithography and etching techniques. The templates had microgroove patterns either 2 μm grooves on 4 μm pitch, or 10 μm grooves on 20 μm pitch. The polymer substrates were 0.5 mm thick polycarbonate (PC) and the embossing was performed in a pressure and temperature controlled press. The press was heated to 166°C and the load was 19 MPa. The temperature and load were maintained for one hour before being cooled to room temperature for ten minutes under load. The embossing duration, temperature, and load used selected using our previously established techniques to ensure that no residual stress remained in the polymer substrate[20-22]. Once cooled to room temperature, the load was released, and the silicon master was removed leaving the micropatterned polymer replicate.

A second embossing process was used to form 50 nm grooves on top of the micron-scale grooves. The master used in this second embossing step was a nickel master with nanogroove patterns. The embossing temperature was 120°C and the load was 27 MPa for 20 minutes. Figure 4.2 shows the second embossing step. The nanogrooves were orientated either parallel or perpendicular to the microgrooves.

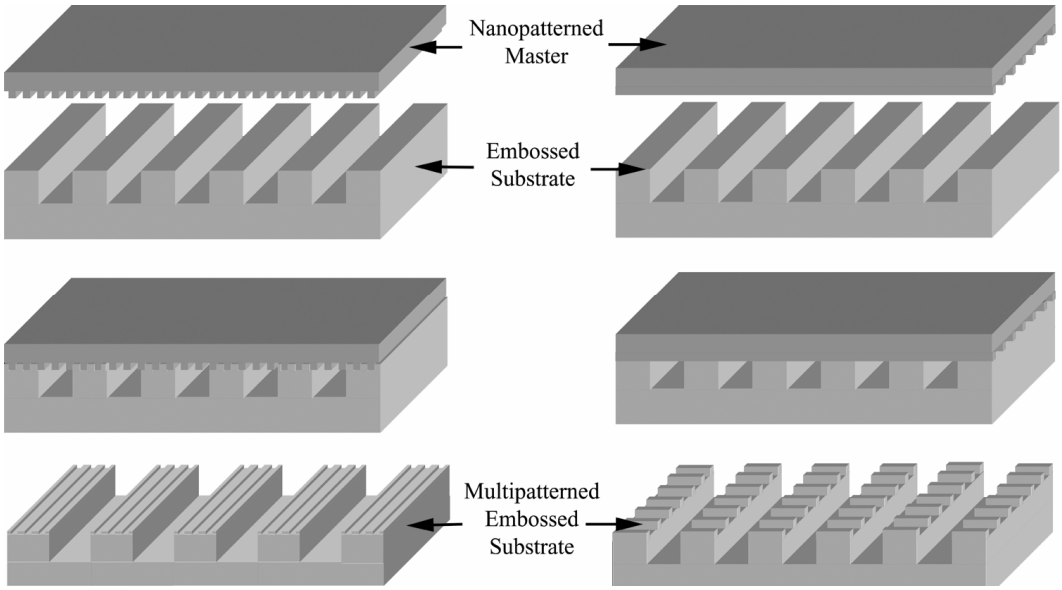

Figure 4.2. Schematic of the second embossing. A nanopatterned nickel master is brought into contact with the micropatterned polymer under lower temperature and higher pressure than the previous embossing process. The mold is than cooled and removed from the substrate leaving nanogrooves on the micromesas.

Substrates were characterized using scanning electron microscopy (SEM) and atomic force microscopy. Figure 4.3 shows embossed samples with nanogrooves running parallel and perpendicular to the microgroove structures. The microgroove depth was 300 nm while the nanogroove depth was 60 nm. The micromesa width increased by about 0.25 μm after the second embossing process. Nanogrooves were 50 nm wide on a 150 nm pitch. To fabricate control samples, a flat silicon wafer performed the second embossing step, which produced a polymer surface identical to the experimental samples, without the nanogrooves.

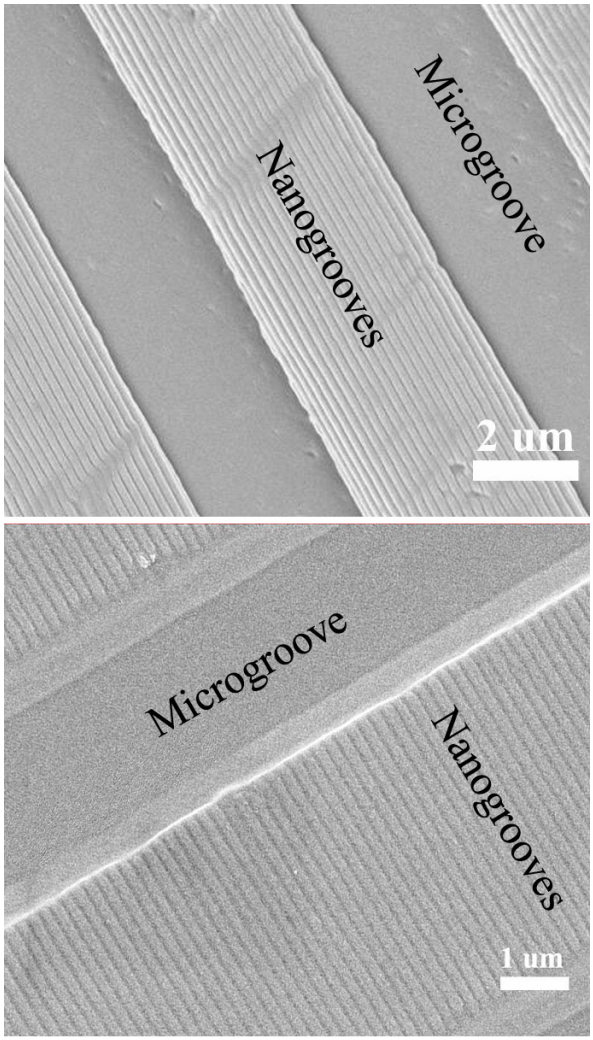

Figure 4.3. Scanning electron micrographs of double embossed substrates. Top image shows nanogrooves on the micromesas running parallel to the microgrooves. Bottom image shows nanogrooves running perpendicular to the microgrooves.

4.2.2 Cell Culture

Finished substrates were coated with 100 Å Ti and 200 Å Au using an electron beam evaporator. The substrates were treated to create a uniform surface chemistry by immersing in hexadecanethiol (HDT) and drying under a nitrogen stream for 15 seconds. Samples were then sterilized using 95% ethanol and rinsed with PBS. Next, the samples were coated with in fibronectin (20 μg/mL in PBS) for 30 minutes followed by an

incubation in 1% heat denatured bovine serum albumin (BSA) at 37°C and 5% CO_2 for 1 hour[23,24]. MC3T3-E1 osteoblast-like cells were then seeded onto the substrates at a density of 50 cells/mm^2. Cells were cultured in α-minimal essential medium with 10% fetal bovine serum and 1% penicillin-streptomycin and incubated at 37°C and 5% CO_2[7].

Samples were then prepared for analysis of cell alignment. After 18 hours in culture, cells were permeablized in 0.5% Triton X-100 cytoskeleton buffer (50 mM NaCl, 150 nM sucrose, 3mM $MgCl_2$, 50 mM tris(hydroxymethyl), 20 μg/mL aprotinin, and 1 μg/mL with pH of 6.8) for 5 minutes and fixed with 3.7% formaldehyde in PBS for 2 min. After a 1-hour incubation in BSA, the samples were incubated in a primary antibody against fibronectin for 1-hour, rinsed twice in PBS, blocked in BSA for 10 minutes and rinsed again with a PBS rinse to prevent non-specific secondary absorption. Samples were next incubated in a secondary fluorochrome labeled anti-IgG, rhodamine-phalloidin and Hoechst DNA stain for 1 hour, rinsed as before and mounted on glass slides.

4.2.3 Analysis

Fluorescent microscopy and image processing software analyzed cell alignment, which was determined by fitting an ellipse to the cell nucleus. The nucleus is a good indication of overall cell alignment[7]. The cell body was also observed to confirm the nucleus alignment. The cell orientation was referenced to the microgroove orientation, resulting in an angle 0-90°. Cells with alignment angles less than or equal to 10° were considered aligned to the microgrooves. Experiments were conducted independently with a minimum of n = 3. Alignment results are reported as mean ± standard error of the

mean. Interactions were tested using an ANOVA with pattern type as the fixed variable using SYSTAT 8.0. *P*-values less than 0.05 were considered significant.

For SEM preparation, samples were removed from culture and rinsed twice in PBS then fixed in 2.5% glutaraldehyde in PBS for 30 minutes at 4°C. Following another rinse in PBS, samples were dehydrated in increasing concentrations (70%, 90% and 100%) of ethanol. Samples were soaked twice in hexamethyldisilazane (HMDS) for 30 minutes each. Samples were left to dry overnight in a desiccator before use in SEM.

4.3 Results and Discussion

Figure 4.4 shows the alignment trends for cells on the fabricated substrates. Alignment to nanogrooves only and a flat control surface is also shown for reference.

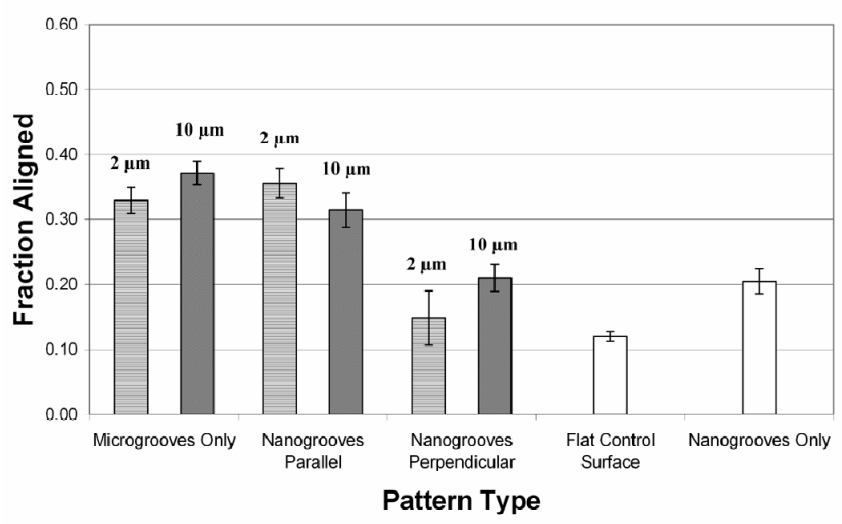

Figure 4.4. Alignment results for cells cultured on micrgrooves only, microgrooves with nanogrooves in parallel, and microgrooves with nanogrooves running perpendicular. Results show alignment trends for microgroove spacings of 2 and 10 µm. Alignment of cells on nanogrooves and a flat control surface is also shown for reference.

The alignment trends are similar for both the 2 and 10 μm wide features. There is no significant difference between microgrooves with embossed flat mesas and those with nanogrooves running in parallel. There is however a decrease in alignment seen on samples with microgrooves and nanogrooves in parallel. This decrease is nearly half of the aligned percentage observed on flat mesa samples. Significant interactions were observed in both micropattern spacings. For 2 μm spacing, ANOVA revealed a p-value equal to 4.11×10^{-3} and a p-value equal to 3.87×10^{-3} for 10 μm spacing.

Most studies of cell response on nanometer scale patterns deal only with nanometer scale topography or roughness[1,13,25-29]. Very few studies have investigated micropatterns of nanometer scale topography or roughness. The studies that have been performed have analyzed nanometer scale pattering with chemical microdomains[15] or patterns of carbon nanotubes[17]. This chapter presents the fabrication of cell substrates with nanometer patterning on well defined micro scale patterns. Patterns such as these represent a more complex cell culture environment that may be able to better mimic *in vivo* conditions. While the results show that cell alignment has a much stronger dependence on the microscale patterns that that of the nanopatterns, a significant decrease in alignment is observed when the nanogrooves run perpendicular to the microgrooves. The drop in cell alignment may be attributed to the interactions between cell extensions on the perpendicular nanopatterns. Figure 4.5 shows an IF image of osteoblast-like cells on a microgrooved surface with perpendicular nanogrooves.

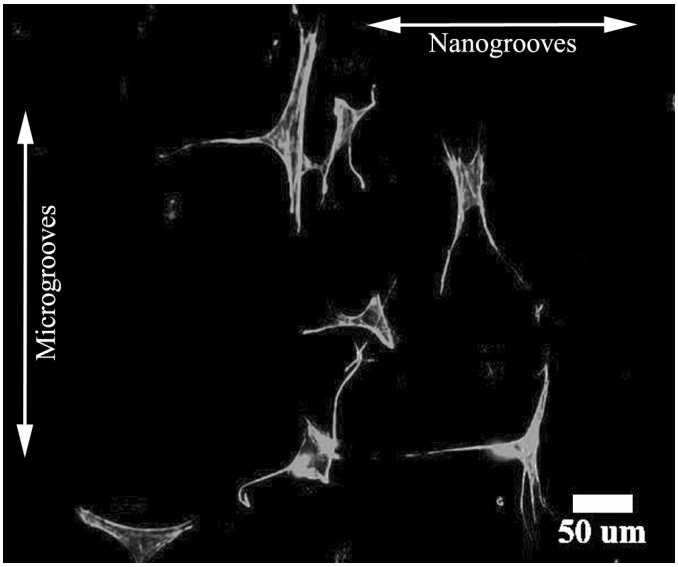

Figure 4.5. IF image of cells on microgrooved surface with nanogrooves running perpendicular. Cell extensions are visible running along the nanogrooves while cell bodies appear to be aligning to the microgrooves.

While the overall cell body appears to align to the microgrooves, cell extensions are visible running perpendicular to the microgrooves along the nanogrooves. These extensions may be sensing the nanogrooves and affecting the overall cell position. Previous studies have examined the extent of filipodia sensing down to 10 nm[26]. SEM was also used to investigate the cell extensions on the nanogrooves. Figure 4.6 shows cell body with an extension running along the nanogrooves.

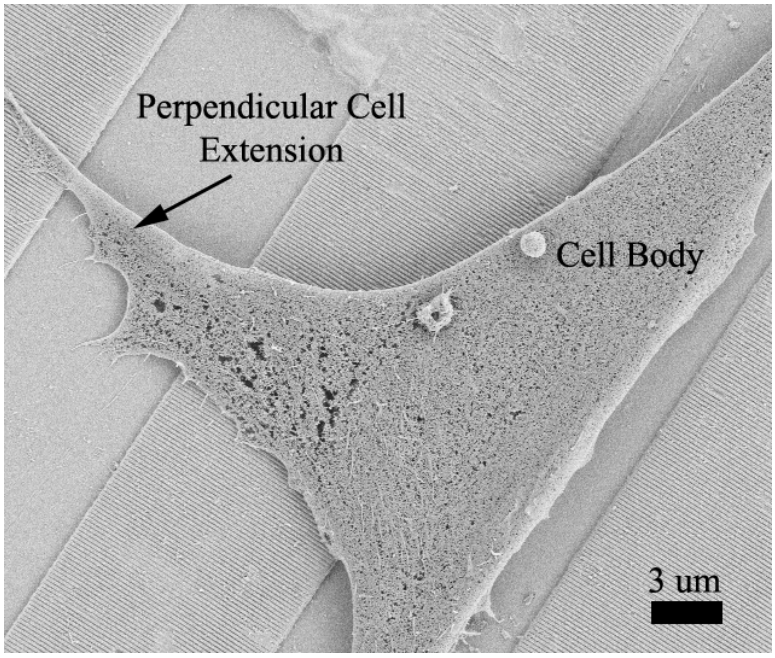

Figure 4.6. SEM image of cell on microgrooves with nanogrooves running perpendicular. Cell extension is seen extending out from the cell body and running along the nanogrooves. Extension also spans groove with no nanopattern to mesa with nanopatterning.

The extension runs along the nanogrooves and spans a microgroove to continue along the nanogrooves. While cell alignment remains nearly constant for samples with flat micromesas and those with nanogrooves in parallel, a significant interaction exists when the nanogrooves are in perpendicular. The cell sensing elements interacting with these perpendicular nanogrooves may be the cause of the reduced alignment.

4.4 Conclusion

This chapter reports the development and fabrication of polymer substrates with combined micrometer-scale and nanometer-scale topography, and explores the response of Osteoblast-like cells to those patterns. The experiments were conduced on two different microgroove spacings with nanogrooves running parallel and perpendicular to

the microgrooves. Samples were treated to obtain a uniform surface chemistry to limit sample variability. Significant differences in cell alignment were observed between samples with nanogrooves running parallel and those running perpendicular. This work presents a technique to fabricate cell substrates with increased pattern complexity to further understand the interactions between cell response and patterning.

4.5 References

1. Flemming RG, Murphy CJ, Abrams GA, Goodman SL, Nealey PF. Effects of synthetic micro- and nano-structured surfaces on cell behavior. Biomaterials 1999;20:573–588.

2. Wilkinson CDW, Riehle M, Wood M, Gallagher J, Curtis ASG. The use of materials patterned on a nano- and micro-metric scale in cellular engineering. Materials Science & Engineering C-Biomimetic and Supramolecular Systems 2002;19(1-2):263-269.

3. Clark P, Connolly P, Curtis ASG, Dow JAT, Wilkinson CDW. Topographical Control of Cell Behavior .1. Simple Step Cues. Development 1987;99(3):439-448.

4. Clark P, Connolly P, Curtis ASG, Dow JAT, Wilkinson CDW. Topographical Control of Cell Behavior .2. Multiple Grooved Substrata. Development 1990;108(4):635-644.

5. Curtis A, Wilkinson C. Topographical control of cells. Biomaterials 1997;18(24):1573-1583.

6. Bhatia SN, Chen CS. Tissue Engineering at the Micro-Scale Biomedical Microdevices 1999;2(2):131-144

7. Charest JL, Bryant LE, Garcia AJ, King WP. Hot embossing for micropatterned cell substrates. Biomaterials 2004;25(19):4767-4775.

8. Dalby MJ, Riehle MO, Yarwood SJ, Wilkinson CDW, Curtis ASG. Nucleus alignment and cell signaling in fibroblasts: response to a micro-grooved topography. Experimental Cell Research 2003;284(2):274-282.

9. Teixeira AI, Abrams GA, Bertics PJ, Murphy CJ, Nealey PF. Epithelial contact guidance on well-defined micro- and nanostructured substrates. Journal of Cell Science 2003;116(10):1881-1892.

10. Thakar RG, Ho F, Huang NF, Liepmann D, Li S. Regulation of vascular smooth muscle cells by micropatterning. Biochemical and Biophysical Research Communications 2003;307(4):883-890.

11. Walboomers XF, Croes HJE, Ginsel LA, Jansen JA. Contact guidance of rat fibroblasts on various implant materials. Journal of Biomedical Materials Research 1999;47(2):204-212.

12. Wan YQ, Wang Y, Liu ZM, Qu X, Han BX, Bei JZ, Wang SG. Adhesion and proliferation of OCT-1 osteoblast-like cells on micro- and nano-scale topography structured pply(L-lactide). Biomaterials 2005;26(21):4453-4459.

13. Yim EKF, Reano RM, Pang SW, Yee AF, Chen CS, Leong KW. Nanopattern-induced changes in morphology and motility of smooth muscle cells. Biomaterials 2005;26(26):5405-5413.

14. Charest JL, Eliason MT, Garcia AJ, King WP. Combined microscale mechanical topography and chemical patterns on polymer cell culture substrates. Biomaterials 2006;27(11):2487-2494.

15. Charest JL, Eliason MT, Garcia AJ, King WP, Talin AA, Simmons BA. Polymer cell culture substrates with combined nanotopographical patterns and micropatterned chemical domains. Journal of Vacuum Science & Technology B 2005;23(6):3011-3014.

16. Middleton JC, Tipton AJ. Synthetic biodegradable polymers as orthopedic devices. Biomaterials 2000;21(23):2335-2346.

17. Zhang X, Prasad S, Niyogi S, Morgan A, Ozkan M, Ozkan CS. Guided neurite growth on patterned carbon nanotubes. Sensors and Actuators B-Chemical 2005;106(2):843-850.

18. Hu W, Yim EKF, Reano RM, Leong KW, Pang SW. Effects of nanoimprinted patterns in tissue-culture polystyrene on cell behavior. Journal of Vacuum Science & Technology B 2005;23(6):2984-2989.

19. Zhang F, Low HY. Ordered three-dimensional hierarchical nanostructures by nanoimprint lithography. NANOTECHNOLOGY 2006;17:1884–1890.

20. Rowland HD, King WP. Polymer deformation and filling modes during microembossing. Journal of Micromechanics and Microengineering 2004;14(12):1625-1632.

21. Rowland HD, King WP, Sun AC, Schunk PR. Simulations of nonuniform embossing: The effect of asymmetric neighbor cavities on polymer flow during nanoimprint lithography. Journal of Vacuum Science & Technology B 2005;23(6):2958-2962.

22. Rowland HD, Sun AC, Schunk PR, King WP. Impact of polymer film thickness and cavity size on polymer flow during embossing: toward process design rules for nanoimprint lithography. Journal of Micromechanics and Microengineering 2005;15(12):2414-2425.

23. Keselowsky BG, Collard DM, Garcia AJ. Surface chemistry modulates fibronectin conformation and directs integrin binding and specificity to control cell adhesion. Journal of Biomedical Materials Research Part A 2003;66A(2):247-259.

24. Keselowsky BG, Collard DM, Garcia AJ. Integrin binding specificity regulates biomaterial surface chemistry effects on cell differentiation. Proceedings of the National Academy of Sciences of the United States of America 2005;102(17):5953-5957.

25. Dalby MJ, Gadegaard N, Riehle MO, Wilkinson CDW, Curtis ASG. Investigating filopodia sensing using arrays of defined nano-pits down to 35 nm diameter in

size. International Journal of Biochemistry & Cell Biology 2004;36(10):2005-2015.

26. Dalby MJ, Riehle MO, Johnstone H, Affrossman S, Curtis ASG. Investigating the limits of filopodial sensing: a brief report using SEM to image the interaction between 10 nm high nano-topography and fibroblast filopodia. Cell Biology International 2004;28(3):229-236.

27. He W, Gonsalves KE, Batina N, Poker DB, Alexander E, Hudson M. Micro/nanomachining of polymer surface for promoting Osteoblast cell adhesion. Biomedical Microdevices 2003;5(2):101-108.

28. Price RL, Ellison K, Haberstroh KM, Webster TJ. Nanometer surface roughness increases select osteoblast adhesion on carbon nanofiber compacts. Journal of Biomedical Materials Research Part A 2004;70A(1):129-138.

29. Wilkinson CDW, Curtis ASG, Crossan J. Nanofabrication in cellular engineering. Journal of Vacuum Science & Technology B 1998;16(6):3132-3136.

CHAPTER 5

CONCLUSION AND FUTURE WORK

5.1 Conclusions

This study seeks to further understand cell response to topographically patterned polymer substrates. Three types of polymer substrates were fabricated using hot embossing and nanoimprint lithography. Cells were cultured on these substrates and cell response observed and quantified. Cell alignment was investigated for all substrates and cell proliferation observed for high-throughput substrates. Results showed significant cell-surface interactions for all substrate types. This work analyzes cell response to patterned substrates to further examine and understand cell-surface interactions

The first type of substrate examined was the high-throughput chip. This substrate featured 35 distinct patterns of grooves and holes with spacing ranging from 1 to 75 μm. A pattern-free, flat control zone was also on the chip for reference measurements. Substrates were fabricated with feature depths of 1 and 5 μm. Results showed a strong dependence upon feature spacing and cell alignment. Smaller spacings showed higher cell alignment than wider spacings. The results also showed significant interactions between feature depth and alignment with deeper features having greater alignment for a given microfeature spacing. Cell proliferation showed no interactions to either feature spacing or feature depth.

The next type of substrate used featured patterned carbon nanotubes. This substrate had carbon nanotube patterns of lines and circles with feature dimensions

ranging from 9 to 76 μm. Cellular alignment was examined on these substrates with significant interactions observed between feature spacing and alignment. SEM analysis also revealed large concentrations of cell extensions interacting with the nanotube patterns. As seen with the high-throughput substrates, cell alignment was stronger at smaller feature spacings.

The third type of substrate used in this work featured combined patterns of micro and nanotopography. These substrates were formed using two embossing steps. The first formed the microgroove topography. The second step used nanoimprint lithography to form nanogrooves on top of the previously formed micromesas. The nanogrooves ran both parallel and perpendicular to the microgrooves. Results for cell alignment on these substrates showed a significant decrease in alignment on patterns of microgrooves with nanogrooves perpendicular. SEM and IF analysis of these samples showed cell extensions moving along the nanogrooves and spanning groove space between sets of nanopatterns.

This work focused in the fabrication of polymer substrates to analyze cell-surface interactions. Substrates ranged from microscale patterning to complex patterns of micro and nanotopographies. Significant interactions were observed in all pattern types examined. The overall lesson seen in this work shows that feature depth plays a significant part in determining cell alignment. While nanotopography can influence cell alignment, the maximum aligned cells were only half of what was observed on deep microgrooves. While the nanopatterned substrates did not have large percentages of aligned cells, significant interactions were still detected. This result is a positive step towards fabricating substrates with patterns over multiple length scales to illicit specific

cell responses. While these systems do not exhibit patterning as complex as that seen in vivo they do provide simple model systems to test cell response. Substrates such as these may enhance the ability to tune cell response for future applications in many biotechnologies.

5.2 Suggestions for Future Work

Suggestions for future work focus on increasing the complexity of the model systems used. Both the substrates and cell model could be changed to further examine cell response. The carbon nanotube substrates used in this work had negligible depth. Future work could focus on partnering the CNT patterning with regular imprint lithography. These substrates could feature carbon nanotube patterns at the bottom of microgrooves or on top of micromesas. This would add another dimension to be examined. The increased number of cell extensions seen on the CNT substrates may guide cell response differently if the patterns are located within a deep groove.

Another avenue for future work to explore is the expansion of pattern size substrates with micro and nanopatterning. This work focused on only one spacing and type of nanopattern. With the advent of electron beam lithography, much more complex nanopatterns can be generated and used as embossing masters. An interesting study would be look at a much larger range of microfeature type and spacing as well as different designs of nanopatterns beyond just grooves.

The cell model used could also be improved to look at more advanced cell function such as differentiation and apoptosis. While the cell model used can be used to test for proliferation, the time span of experiment may have affected results. More

advanced cell models can test for higher order cell functions that may be affected using the substrates and fabrication methods talked about within this thesis. *In vivo* testing is another avenue for future work. As the overall goal of emerging biotechnologies is the successful incorporation of the an implant into the body, *in vivo* testing is crucial to examine cell response as compared to *in vitro* conditions. The *in vivo* response will ultimately be the determining factor for a successful biotechnology.